To the Graduate Council:

I am submitting herewith a dissertation written by Corey L. Moses entitled "Effects of Applied Pressure and Polymer Architecture on the Second Virial Coefficient of Polystyrene Solutions." I have examined the final copy of this dissertation for form and content and recommend that it be accepted in partial fulfillment of the requirements for the degree Doctor of Philosophy with a major in chemistry.

W. Alexander Van Hook, Major Professor

We have read this dissertation
and recommend its acceptance:

Accepted for the Council:

Vice Provost and
Dean of the Graduate School

Effects of Applied Pressure and Polymer Architecture on the Second Virial Coefficient of Polystyrene Solutions

A Dissertation
Presented for the
Doctor of Philosophy Degree
The University of Tennessee, Knoxville

Corey L. Moses
August 2001

Dedication

To my parents, Nelson and Carol Moses, for their tireless, loving encouragement during my life and especially during the preparation of this manuscript.

Acknowledgment

I am very fortunate to have worked under the guidance of Prof. W. Alexander Van Hook. By his insightful approach to solving problems coupled with his broad knowledge of polymer solution thermodynamics, he taught me to think critically and motivated me to work tenaciously toward this project's completion. By his close scrutiny of this document and other manuscripts, he also taught me to be a better writer.

Special thanks go to my committee, Prof. Jeffrey Kovac, Prof. Lee Magid, and Prof. Paul Phillips, for their helpful suggestions and careful review of this dissertation. Thanks also to Dr. Attila Imre for teaching me about static light scattering, for sharing your knowledge of the current literature, and for your friendship. To Dr. Luis Rebelo, who played a major role in the design and construction of the osmometer and osmometry cells, I appreciate your willingness to help me interpret my results and troubleshoot the instrument. To Dr. Brian Taylor, Phil Stimac, Angela Whisnant, and Jason Pittman, thank you for your friendship.

I must also thank John Nelson and Art Pratt, who spent countless hours constructing or repairing instruments and glassware for my use. Your work made mine possible.

Above all, I thank the Lord Jesus Christ for his presence in my life. *I can do all things through Christ who strengthens me. Philippians 4:13.*

Abstract

Second virial coefficients (A_2) of dilute polystyrene (PS) solutions in good, theta (θ) and poor solvents have been measured as a function of applied pressure using membrane osmometry and static light scattering. Membrane osmometry and static light scattering equipment, designed to function at pressures in the range ($0.1 \leq P/MPa \leq 6.0$) and ($0.1 \leq P/MPa \leq 35.0$), respectively, have been used in these measurements, and the resulting pressure coefficients (dA_2/dP) are measures of the effect of pressure on solvent quality. For the system PS/toluene, membrane osmometry and SLS-obtained values of dA_2/dP are compared.

The effect of polymer architecture on the second virial coefficient has also been studied with static light scattering measurements on linear(L)-star(S) polystrene solutions at atmospheric pressure. Second virial cross coefficients between linear and star polystyrenes of similar molecular weight ($A_{2(L-S)}$) quantify the extent of linear-star PS interaction in good, θ, and poor solvents. Linear-star polystyrene interactions are preferred to polystyrene-solvent interactions in the good solvent (toluene). However, in θ (cyclohexane) and poor (MCH) solvents, there is no difference between linear-star and polystyrene-solvent interactions.

Table of Contents

Chapter	Page
1. Introduction	1
A. Second Virial Coefficient	2
B. Membrane Osmometry	6
C. Static Light Scattering	10
D. Second Virial Cross Coefficient	14
2. Experimental	18
A. Materials and Sample Preparation (Membrane Osmometry)	18
B. Membrane Osmometry Cell	18
C. Membrane Osmometer	21
D. Typical Membrane Osmometry Experiment	23
E. Materials and Sample Preparation (SLS)	23
F. SLS Cell	28
G. Cloud Point Measurements	31
3. Results	33
A. Membrane Osmometry	33
B. Pressure Coefficient of the Second Virial Coefficient from Membrane Osmometry	38
C. Pressure Coefficient of the Second Virial Coefficient from Static Light Scattering	41

Chapter **Page**

D. Second Virial Cross Coefficients Between Linear and Star Polystyrenes 50

E. Cloud Points of Linear and Star Polystyrenes in Cyclohexane and Methylcyclohexane 55

4. Discussion 58

A. Pressure Coefficient of the Second Virial Coefficient of Polystyrene in Organic Solvents 62

B. Second Virial Coefficients and Second Virial Cross Coefficients of Linear and Star Polystyrene Systems 71

5. Conclusion 74

References 77

Appendices 82

Appendix 1 83

Appendix 2 91

Vita 101

List of Tables

Table		Page
2-1	Solvents Used in Membrane Osmometry	19
2-2	Solvents Used in SLS	24
2-3	Polystyrene Samples Used in SLS	25
2-4	Polystyrene Solutions Used in SLS	26
2-5	Solutions Used in Cloud Point Measurements	32
3-1	Second Virial Coefficients and Pressure Coefficients of Second Virial Coefficients of Polystyrene Dissolved in Various Organic Solvents	48
3-2	Second Virial Coefficients of Linear and Star Polystyrene Solutions	51
3-3	Initial and Fit Parameters to Determine Second Virial Cross Coefficients	54

List of Figures

Figure		Page
1-1	Upper and lower critical solution temperature branches in a polymer solution	5
1-2	Osmosis through a semipermeable membrane	7
1-3	Phase diagram of a polydisperse polymer solution	16
2-1	Membrane osmometry cell	20
2-2	Membrane osmometer	22
2-3	SLS experimental set-up	27
2-4	SLS cell	29
3-1	Developing osmotic pressure of 1% (w/w) PS 100k in toluene as a function of time and applied pressure	34
3-2	Developing osmotic pressure of 3% (w/w) PS 100k in toluene as a function of time and applied pressure	36
3-3	Developing osmotic pressure of 5% (w/w) PS 100k in toluene as a function of time and applied pressure	37
3-4	Osmotic pressure of 1% (w/w) PS 100k in toluene as a function of applied pressure	40
3-5	Scattering intensity of PS 90k in toluene as a function of applied pressure (0.1 to 6.0 MPa)	42
3-6	Second virial coefficient of PS 90k in toluene from 0.1 to 6.0 MPa	43

Figure **Page**

3-7 Second virial coefficients of polystyrene in various organic solvents near 25 °C as a function of applied pressure 45

3-8 Second virial coefficient of PS 25k in CH from 22 - 45°C as a function of applied pressure 46

3-9 Second virial coefficients of PS 400k and PS 900k in CH near 30°C as a function of applied pressure 47

3-10 Second virial coefficients of linear PS 400k and 8-arm star PS 417k mixtures in (A) toluene, (B) CH, and (C) MCH 53

3-11 Cloud point temperatures of polystyrenes in CH 56

3-12 Cloud point temperatures of linear and 8-arm star polystyrenes in MCH . . 57

4-1 SLS dA_2/dP of PS/toluene 65

4-2 SLS dA_2/dP of PS/chloroform 66

4-3 dA_2/dP of PS/decalin as a function of solvent composition 68

Chapter 1

Introduction

In 1887, Jacobus Henricus van't Hoff stated that the osmotic pressure (Π) of an ideal dilute solution was analogous to the pressure (P) exerted by an ideal gas and that the same laws of thermodynamics were applicable in both cases.[1] Osmotic measurements of rubber in various solvents made by Posnjak[2] prompted Ostwald and Mündler[3] to recast van't Hoff's equation to account for the nonideality of the solution caused by the swelling pressure of the rubber. Schultz,[4] considering osmotic pressure measurements made by Adair[5] on aqueous hemoglobin solutions, suggested that a plot of Π/c against c (c = solute concentration) should be linear with a y-intercept proportional to the reciprocal molecular weight of the polymer. Haller[6] then showed that earlier osmotic work by Duclaux and Wollman[7] with cellulose nitrate solutions and by Caspari[8] with rubber in benzene actually did show a linear relationship between Π/c and c. Haller[6] went on to propose the existence of the second osmotic virial coefficient (A_2) in terms of the excluded volume integral.

There is a large body of literature pertaining to second virial coefficients. One of the more extensive lists compiled by Brandrup[9] contains data on at least 100 polymer solutions over the temperature range 5-125 °C at atmospheric pressure. He reports data for only two systems (polystyrene/cyclohexane, polystyrene/decalin) at pressures (P) in excess of atmospheric ($0.1 \leq P/MPa \leq 80$) and these were measured by Lechner and Schultz[10] from static light scattering (SLS) measurements. Gaeckle and Patterson[11] have studied pressure-dependent second virial coefficients by SLS (polystyrene in 2-butanone

and polyisobutylene in 2-methylbutane, $0.1 \leq P/MPa \leq 11$). The pressure dependences they report are small— on the order of at most a few percent of an already small effect— or nearly zero for most solutions. A few other groups[12-15] have reported SLS second virial coefficients of polymer/organic solvent systems at high pressure.

To our knowledge, only Charmasson and Catella[16] have reported membrane osmotic pressures of polymer solutions under pressure. They report that the sign of $d\Pi/dP$ over the applied pressure range 0.1 - 50 MPa changes from negative to positive (-10^{-4} MPa/MPa $\leq d\Pi/dP \geq +10^{-4}$ MPa/MPa) according to solution composition for concentrated solutions (22-35 wt. %) of polyvinylpyrrolidone (20,000 g/mol) in a mixture of water and methanol. They also report the pressure coefficient ($d\Pi/dP$) of moderately-concentrated dextran (40,000 g/mol) in water to be small and positive ($\sim 10^{-5}$ MPa/MPa) and of the same order of magnitude reported in this work for a dilute solution of polystyrene in toluene up to 6.0 MPa applied pressure.

A. Second Virial Coefficient

The second virial coefficient (A_2) is a measure of polymer-polymer interaction in dilute solution and may be expressed in terms of the change in chemical potential of the solvent, ($\partial\mu_I/\partial c$), with respect to polymer concentration (c). Subscript I refers to solvent, and (later) subscript II will refer to polymer:

$$\left[\left(\frac{\partial \mu_I}{\partial c}\right)_{T,P} = \left[(\text{constant})\left(\frac{1}{M} + 2A_2c + 3A_3c^2 + \ldots\right)\right]\right] . \qquad (1\text{-}1)$$

M is the polymer molecular weight and A_3 is the third virial coefficient. In dilute solution, the series is usually truncated after the term containing the second virial coefficient. The first term applies to an infinitely dilute solution in which there are no polymer-polymer interactions. The term containing the second virial coefficient accounts for polymer-polymer interactions in the concentration range (infinite dilution $\leq$ c $\leq$ dilute solution).[17]

When $A_2 > 0$, polymer-solvent interactions are preferred over polymer-polymer interactions and the solvent is considered good. Each polymer chain can be thought to occupy a distinct volume element in the solution such that there is no overlap with other polymer molecules. Flory[18] called this behavior the excluded volume effect and used a hard-sphere model to describe the behavior of the solvated polymer molecules. The size of the chain, as measured by the root mean square end-to-end distance ($<R^2>^{1/2}$), scales as a function of molecular weight (M) in a good solvent such that the chain is often described as "swollen".[19-20]

$$\langle R^2 \rangle^{1/2} \sim M^{0.6} \qquad (1\text{-}2)$$

Conversely, polymer-polymer interactions are preferred when the solvent is poor. In this case, $A_2 < 0$ and the chains are collapsed. Solutions with large negative second virial coefficients are unstable and separate into solvent-rich and polymer-rich phases.[19]

If polymer-polymer and polymer-solvent interactions are equally favorable, $A_2 = 0$ and the solvent is a theta (θ) solvent. Flory and Krigbaum[21] showed that in a θ solvent, the chains take on ideal dimensions (neither swollen nor collapsed), the excluded volume goes to zero, and the solution is considered ideal. Imre and Van Hook[22] have shown from liquid-liquid demixing data gathered from polystyrene solutions that solvent quality is also

sensitive to pressure, especially in the θ–to-poor solvent quality region, and that pressure may be used to convert some poor solvents to θ solvents, and vice versa.

The pressure derivative of the second virial coefficient, dA_2/dP, can be used to determine how solvent quality changes with pressure and is related to the pressure derivative of the upper critical solution temperature (UCST), another solvent quality index. Negative values of dA_2/dP correspond to positive values of dT_{UCST}/dP and vice versa. Typically, solutions of polymers dissolved in θ solvents have separated upper and lower critical temperature branches, a region in [reciprocal critical temperature $(1/T)_{CR}$, reciprocal-square-root molecular weight $(1/M)^{1/2}$] space which represents a homogeneous, one-phase solution. The solution is two-phase (demixed) above and below the upper and lower critical branches, respectively. As solvent quality progresses from θ to good, the distance between upper and lower critical solution temperature branches increases; consequently, the area of the one-phase region also increases. Figure 1-1 shows the case in which applied pressure improves solvent quality. (Curves labeled P1 are at atmospheric pressure, and those labeled P2 are some higher pressure (P2 > P1).) Good solvent systems have larger one-phase solubility regions than θ solvent systems, and in some solutions UCST or LCST may be experimentally inaccessible.[23-24]

The second virial coefficient, A_2, is routinely obtained from osmotic pressure or static light scattering measurements, and we have modified these techniques to study the effect of pressure on A_2.

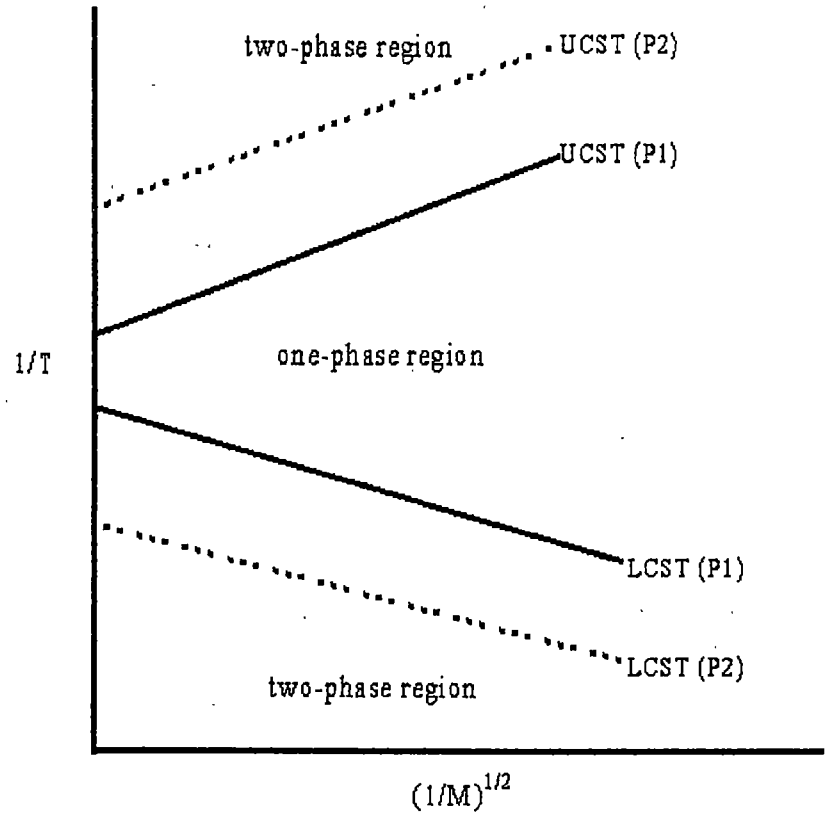

Figure 1-1. Upper and lower critical solution temperature branches in a polymer solution.

Pressure 1 (P1) = 0.1 MPa < P2.

B. Membrane Osmometry

Osmosis is the process by which pure solvent passes through a semipermeable membrane (one which permits the passage of solvent but prohibits the passage of solute) into a solution, and the pressure that must be applied to stop this flow is the osmotic pressure, Π. Osmotic pressure is a measure of solvent chemical potential. At equilibrium, the chemical potential of the pure solvent at a pressure P, ($\mu_I^0(P)$), is equal to the chemical potential of the solvent in solution ($\mu_I(P + \Pi)$).[25] This situation is shown in Figure 1-2; the semipermeable membrane is represented by the vertical, dashed line.

Taking into account the presence of the solute (written in terms of mole fraction of solvent $X_I = 1 - X_{II}$), the equilibrium between pure solvent and solvent in the solution may be expressed

$$\mu_I^{\circ}(P) = \mu_I(X_I, P + \Pi) \tag{1-3}$$

where

$$\left[\mu_I(X_I, P + \Pi) = \mu_I^{\circ}(P + \Pi) + (RT \ln X_I) + \mu_I^{ex}(X_I, P)\right] \tag{1-4}$$

in which R is the ideal gas constant, T is temperature in Kelvin, and $\left[\mu_I^{ex}(X_I, P)\right]$ is the excess chemical potential of solvent in solution.[25] When the solution is ideal, $\mu_I^{ex}(X_I, P) = 0$. Considering the effect of applied pressure on the osmotic pressure of an ideal solution, the pure solvent term in equation (2) may be expanded

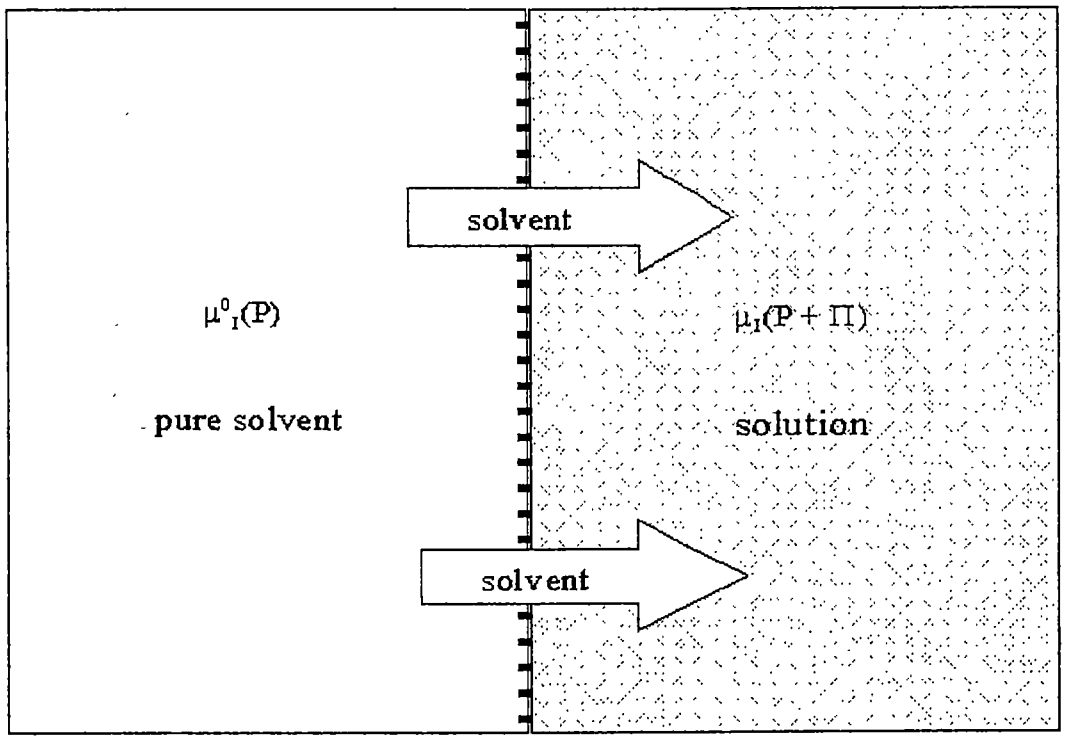

Figure 1-2. Osmosis through a semipermeable membrane.

$$\left[\mu_I^{\circ}(P+\Pi) = \mu_I^{\circ} + \int_P^{P+\Pi} \overline{V}_I^0 dP\right] \tag{1-5}$$

since

$$\left[\left(\frac{\partial \mu_I^{\,0}}{\partial P}\right)_T = \left(\overline{V}_I^0\right)\right] . \tag{1-6}$$

$\overline{V}_I^0$ represents the molar volume of pure solvent.[25] Therefore,

$$\mu_I(X_I, P+\Pi) = \mu_I^{\,0} + \overline{V}_I^0\Pi + RT\ln X_I . \tag{1-7}$$

Since $\mu_I(X_I, P + \Pi) = \mu_I^{\,0}$ at equilibrium,

$$\overline{V}_I^0\Pi = \left[-\left(RT\ln X_I\right)\right] . \tag{1-8}$$

If the solution is dilute, $\ln X_I$ may be replaced by $\ln(1-X_{II}) \cong -X_{II}$ where X_{II} is the mole fraction of solute, in which case equation (1-8) simplifies to[25]

$$\left(\overline{V}_I^0\Pi\right) = \left[\left(RT\, X_{II}\right)\right] . \tag{1-9}$$

Equation (1-9) may be rewritten in terms of the total volume of the solvent (V) and moles of solute in solution (n_{II}) where $V = n_I\overline{V}_I^0$, n_I = moles of solvent in solution, and $n_{II} \cong X_{II}\, n_I$:

$$\Pi = \left(\frac{n_{II}}{V}RT\right) . \tag{1-10}$$

The term $\frac{n_{II}}{V} = \frac{c}{M_n}$ where c = weight of solute/volume of solvent and M_n is the number-

averaged molecular weight of the polymer[25] ($M_n = \frac{\Sigma N_x M_y}{\Sigma N_x}$; N_x = total number of molecules of length x, M_y = molecular weight of a molecule of degree of polymerization y);[19] therefore,

$$(\Pi) = \left(\frac{c}{M_n}RT\right). \tag{1-11}$$

Equation (1-11) is the van't Hoff equation and is applicable to ideal dilute solutions; however, polymer solutions, even dilute ones, do not behave ideally.[25] In this case, $\left[\mu_I^{ex}(X_I, P)\right] \neq 0$. It is conventional to express the excess chemical potential term in virial expansion form such that

$$\left[\mu_I\left(X_I, P+\Pi\right)\right] = \left[\mu_I^{\circ}(P+\Pi) + \left(RT \ln X_I\right) + (RT)[A_2(P,T)X_I + A_3(P,T)X_I^2 + ..\right]. \tag{1-12}$$

A_2 and A_3, the second and third virial coefficients, respectively, account for higher-order polymer-polymer interactions that cause solution behavior to deviate from ideality and are functions of pressure and temperature. In the dilute solution approximation (i.e. $\ln(1-X_{II}) \cong -X_{II}$),

$$\left\{\left[\left(\overline{V}_I^0 \Pi\right)\right] = \left[(RT)\left(X_{II} + A_2(P,T)X_{II} + A_3(P,T)X_{II}^2 + ...\right)\right]\right\}. \tag{1-13}$$

Most texts use concentration (c) in place of mole fraction (X), and we will adhere to that practice in arriving at an expression for the osmotic pressure of a dilute, non-ideal polymer solution:

$$\Pi = (RTc)\left(\frac{1}{M_n} + A_2 c + A_3 c^2 ...\right). \tag{1-14}$$

The first term (RTc/M_n) gives the osmotic pressure in the limit of zero polymer concentration, and higher terms (RTc^2A_2/M_n , RTc^2A_3/M_n) account for polymer-polymer interactions. If the solution is sufficiently dilute, equation (1-14) may be truncated after the term containing the second virial coefficient.[25]

C. Static Light Scattering

Pure liquids scatter light because of small fluctuations in refractive index, and hence local density, over time. Consider two small, equally-sized volume elements in a liquid. At any instant, there are usually different numbers of molecules in each volume element, so the intensity of light scattered from these elements is not the same. The fraction of scattering not cancelled by interference is the light scattered by the pure liquid.[17]

Light scattered from a dilute polymer solution consists of scattering not only by the solvent but also by the polymer dissolved in the solvent. If the polymer solution were ideal, the intensity of light scattered by a unit volume of solution from an angle of observation θ would be written[26]

$$\left(i_{u,\theta}\right) = \left(\frac{I_0(1+\cos^2\theta)\left(2\pi^2 n_0^2\right)(dn/dc)^2 c}{\lambda^4 r^2[-(1/V_I kT)(\partial\mu_1/\partial c)_{T,P}]} \right) \qquad (1\text{-}15)$$

I_0 is the incident laser beam intensity, $\pi = 3.1415\ldots$, n_0^2 is the squared refractive index of the pure solvent, c is concentration, r is the distance between the detector and the scattering volume, λ is the wavelength of the laser in vacuum (633.4 nm), k is Boltzmann's constant, and T is temperature (Kelvin). dn/dc, the refractive index

increment, is the change in the refractive index of the solution with respect to change in polymer concentration. When the solution is dilute,

$$\left[\left(\frac{-1}{V_I kT}\right)\left(\frac{\partial \mu_I}{\partial c}\right)_{T,P} = (N_A)\left(\frac{1}{M} + 2A_2 c + 3A_3 c^2 + \ldots\right)\right] \qquad (1\text{-}16)$$

(N_A = Avogadro's Number) and

$$\left[\left(i_{u,\theta}\right) = \left[\left(I_0(1+\cos^2\theta)\frac{2\pi^2 n^2}{r^2 \lambda_0^4 N_A}\left(\frac{dn}{dc}\right)^2 c \frac{1}{M^{-1} + 2A_2 c + 3A_3 c^2 + \ldots}\right)\right]\right]. \qquad (1\text{-}17)$$

The virial expansion may be truncated after the second term $(2A_2 c)$. n_0^2(from equation (1-15)) has been replaced by n^2 (squared refractive index of the solution) because $n^2 \cong n_0^2$ in dilute solution. (For a 1% (w/w) solution, $\left(\frac{n^2 - n_0^2}{n^2}\right) \cong \left(\frac{n^2 - n_0^2}{n_0^2}\right) \leq 3\text{x}10^{-6}$, which is negligible.[17, 26])

The intensity of light scattered by a unit volume of solution depends not only on the angle of observation but also on incident laser beam intensity (I_0) and the distance between the detector and the scattering volume (r). These instrumental parameters are conveniently combined with scattering intensity to yield the Rayleigh ratio, (R_θ), which is independent of scattering angle[17]:

$$R_\theta = \left(\frac{i_{u,\theta} r^2}{I_0(1+\cos^2\theta)}\right) = \left(\frac{Kc}{M_w^{-1} + 2A_2 c + 3A_3 c^2 + \ldots}\right). \qquad (1\text{-}18)$$

K is an optical constant ($K = \frac{2\pi^2 n_0^2}{\lambda_0 N_A}\left(\frac{dn}{dc}\right)^2$) and M_w is the weight-averaged molecular weight of the polymer ($\left(M_w\right) = \left(\frac{\Sigma N_x M_y^2}{\Sigma N_x M_y}\right)$).[19] The difference between Rayleigh ratios of solution and pure solvent ($R_{\theta,\ solution} - R_{\theta,\ solvent}$) is the excess Rayleigh ratio (R_θ^{ex}), and it is this quantity that contains the contribution of dissolved polymer to the absolute scattering intensity of the solution (i).[17]

Second virial coefficients as well as polymer molecular weights and radii of gyration may be determined from Zimm analysis of scattered light intensities. The basis of the Zimm method is equation (1-19):

$$\frac{Kc}{R_\theta} = \left[\left(\frac{1}{M_w}\right)\left(1 + \frac{R_g^2 q^2}{3}\right) + \left(2A_2 c\right)\right] \qquad (1\text{-}19)$$

in which R_g is the z-average (the zero-concentration limiting value) root-mean-square radius of gyration and q is the magnitude of the scattering wave vector equal to $(4\pi n_0/\lambda_0)\sin(\theta/2)$. A set of experimentally-determined Kc/R_θ ratios at different concentrations and angles of observation are plotted against $\sin^2(\theta/2)$ to produce the grid-like Zimm plot. Extrapolations are made to zero concentration and to zero angle. The second viral coefficient is proportional to the initial slope of the line extrapolated to zero angle.[17, 19]

Second virial coefficients may be obtained from Zimm or Debye plots of scattering intensity or from membrane osmometry. Zimm plots are constructed from data collected at three or more scattering angles(θ); Debye plots, from Kc/R_θ, concentration data

collected at only one angle (usually $\theta = 90$). Osmotic pressure is related to static light scattering through Debye theory in which

$$\frac{Kc}{R_0} = \frac{1}{M_w} + (2A_2c) + \ldots = \frac{\Pi}{RTc} \qquad (1\text{-}20)$$

where R_0 is the excess Rayleigh ratio at zero scattering angle which is determined from extrapolation of $R_\theta = (I_s/I_0)[r^2(1+\cos^2\theta)$ for a measured set of R_θ's to zero angle, $\theta = 0$.[26-28] (I_s and I_0 are the scattered and incident light intensities, respectively, and r is the distance from the center of the scattering volume to the detector.[26-28]) Therefore, it is possible to compare second virial coefficients obtained from membrane osmometry to those from static light scattering. Both of these techniques have been used extensively to study the effect of temperature on A_2; however, there is relatively little work reported in the literature on the effect of pressure on A_2. Most membrane osmometry and static light scattering studies have been conducted at atmospheric pressure because A_2 is small and difficult to measure accurately and precisely. The change in the second virial coefficient with pressure (dA_2/dP) is smaller and even more difficult to measure without considerable attention to osmometry and light scattering cell design as well as to experimental protocol. However, we have designed equipment and developed techniques to make these measurements, via membrane osmometry and static light scattering at externally-applied pressures in excess of atmospheric. The majority of this work is devoted to the study of dA_2/dP in dilute, linear polystyrene solutions by SLS and membrane osmometry. It is our hope that this information will permit us to augment the small body of published work on

the effect of pressure on A_2 and to refine the interpretation of the influences of pressure and temperature on demixing data gathered in this laboratory by light scattering.

D. Second Virial Cross Coefficient

In a smaller, related study, we have used SLS to determine how polymers of similar chemical structure but dissimilar architecture interact in dilute solution. The relative strength of interaction between such polymers can be ascertained from the value of the second virial *cross* coefficient. Just as the second virial coefficient is a measure of the extent of like-polymer interaction in (one solvent + one polymer) solutions, the second virial *cross* coefficient quantifies interactions between (architecturally) dissimilar polymers in (one solvent + polymer 1 (architecture 1) + polymer 2 (architecture 2)) solutions. Second virial cross coefficients may be obtained from membrane osmometry or static light scattering, and we have used the latter technique in this work.

A general explanation of light scattering in multicomponent systems was developed by Stockmayer.[29] The intensity of light scattered from a dilute solution of two different polymers (a,b) is a function of interactions between identical (aa, bb) and nonidentical (ab) polymer molecules and may be expressed in terms of the excess Rayleigh ratio (as previously discussed) at zero scattering angle, R_0. The (overall) second virial coefficient of the solution, A_2, is some combination of contributions from $A_{2(a\text{-}a)}$, $A_{2(b\text{-}b)}$, and the second virial cross coefficient $A_{2(a\text{-}b)}$.[17]

We have used static light scattering to measure second virial cross coefficients ($A_{2(L\text{-}S)}$) of (linear (L) polystyrene + 8-arm star (S) polystyrene) systems in good, θ, and

poor solvents (toluene, CH, and MCH, respectively) and compare our results to membrane osmometry data reported by Striolo and Prausnitz[30] for similar polystyrene solutions. This information will allow us to determine how much $A_{2(L\text{-}S)}$ contributes to the second virial coefficient of the solution, A_2, and how that contribution is influenced by solvent quality.

We were concerned about the effect of polymer solubility on the second virial cross coefficients. Are linear and 8-arm star polystyrene solubilities different, and how large must the difference be to affect $A_{2(L\text{-}S)}$ significantly? To answer such questions, we measured cloud points of linear polystyrenes and 8-arm star polystyrenes in CH and in MCH (1 polymer + 1 solvent systems). The cloud point (CP) is defined in terms of the temperature and pressure, $(T,P)_{CP}$, at which precipitation first occurs;[24] however, we will refer only to cloud point *temperatures* because all measurements were made at atmospheric pressure.

Consider the polymer solution phase diagram in Figure 1-3. As a one-phase solution (F) is slowly cooled, it reaches a point (G) on the cloud point curve (B) at which it becomes turbid. This turbidity results from the onset of precipitation. If the solution is cooled further, it will pass through a metastable one-phase region (C) before reaching the unstable two-phase region (E). The cloud point curve (B) is the boundary between stable (F) and metastable (C) regions, and the spinodal curve (D) separates the unstable (two-phase) region (E) from the metastable region. When the polymer is monodisperse ($M_w/M_n = 1$), the critical solution point (A) and the maximum in the cloud point curve are

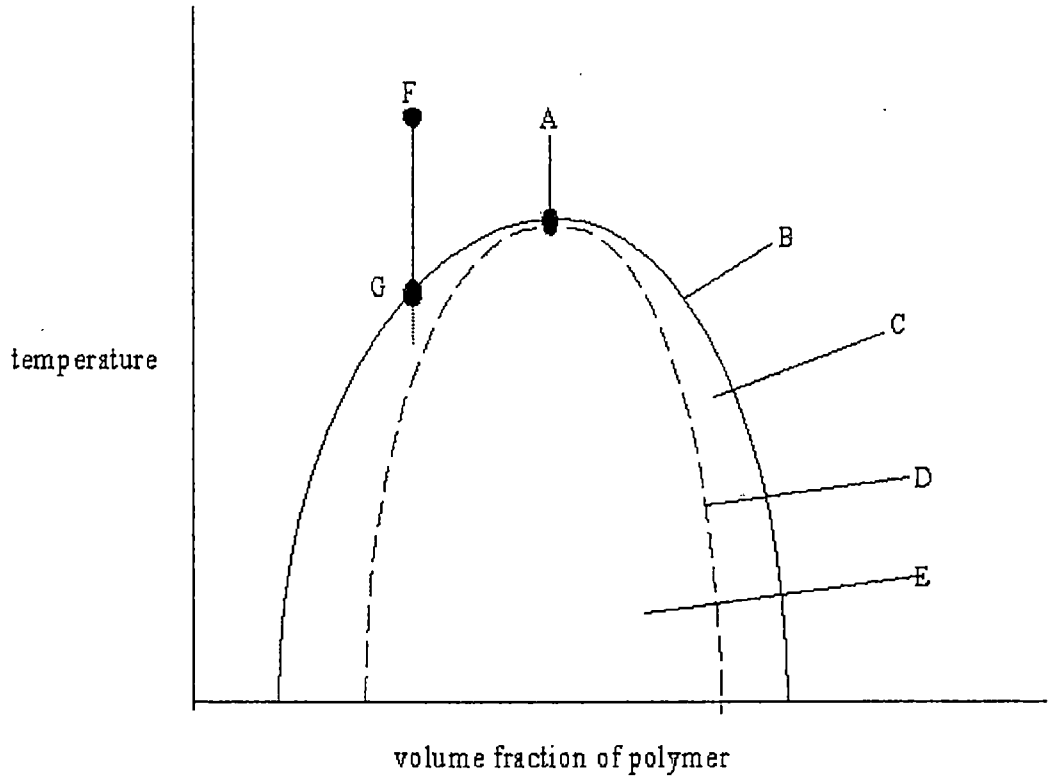

Figure 1-3. Phase diagram of a polydisperse polymer solution.

Key:
A. Critical solution point
B. Cloud point curve
C. Metastable region
D. Spinodal curve
E. Unstable (two-phase) region
F. Point in stable (one-phase) region
G. Cloud point

coincident. When M_w/M_n is only slightly greater than one (polydispersity is low), the difference between the critical solution point and the cloud point maximum is small. In such (real solution) cases, the cloud point maximum can be substituted for the critical solution temperature without significant error.[24, 31]

Cloud points are commonly measured from visual inspection or from changes in the transmission pattern of a laser shining through the solution as it is slowly cooled or heated.[31] We have used visual observation with platinum resistance thermometry to measure cloud point temperatures for linear and star polystyrenes of various molecular weights in CH and MCH. This information will enable us to determine how solubility differences between architecturally dissimilar polymers in solution affect the value of the second virial cross coefficient.

Chapter 2

Experimental

A. Materials and Sample Preparation (Membrane Osmometry)

Osmotic pressure measurements were made on 1-5% (w/w) polystyrene (PS) in toluene, cyclohexane (CH), and methylcyclohexane (MCH) and on 3% (w/w) polystyrene in butyl acetate at ambient temperature (22-25 °C). Solvent characteristics are listed in Table 2-1. Polystyrene samples (M = 100,000g/mol, M_w/M_n = 1.1) were purchased from Pressure Chemical Company. Dry cellulose acetate membranes with molecular weight cut-off of 10,000 g/mol were purchased from Jupiter Instrument Company, conditioned to the solvent,[32] and trimmed before use.

B. Membrane Osmometry Cell

The osmometry cell is shown in Figure 2-1. It consists of a pair of stainless steel disks, each with a shallow cylindrical cavity (shaded portions; cavity diameter approximately 3.8 cm) containing either solvent or solution. The combined cavity volume of both pieces is approximately 15 mL.

The membrane is held between perforated stainless steel supporting plates held between the disks using "O" ring seals. One supporting plate has two small shoulders that grip the membrane. Each plate contains more than 100 small holes (average hole diameter = 1/16 inch) which permit solvent to diffuse across the membrane.

Table 2-1

Solvents Used in Membrane Osmometry

Solvent	Source	Purity
toluene	Fisher Scientific	99.8 %
cyclohexane	Aldrich Chemical Company, Inc.	99.5%, anhydrous
methylcyclohexane	Aldrich Chemical Company, Inc.	99% pure, anhydrous
butyl acetate	Aldrich Chemical Company, Inc.	99.5% pure, A.C.S. reagent grade

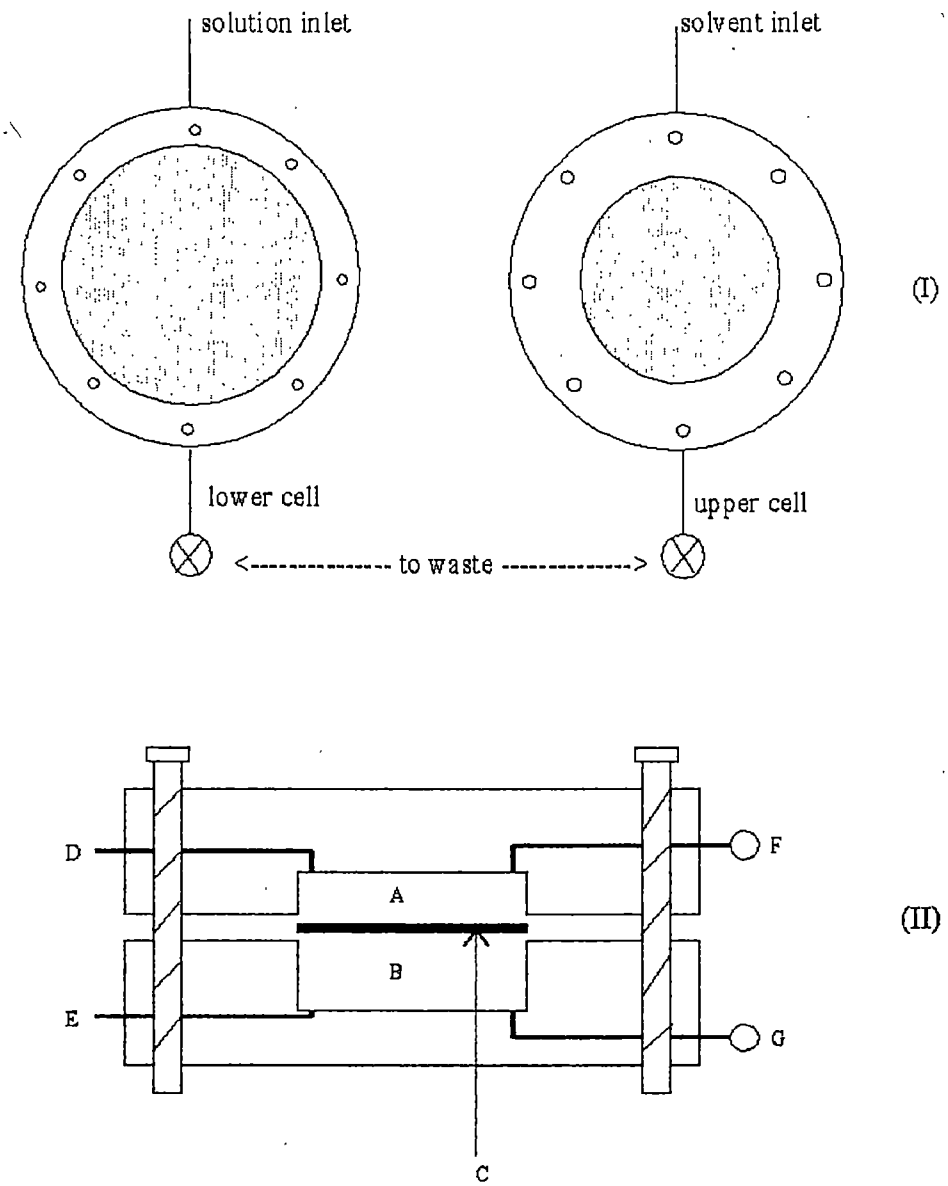

Figure 2-1. Membrane osmometry cell. (I) solvent and solution compartments; (II) in cross section (Key: A. solvent compartment, B. solution compartment, C. membrane held between membrane plates, D. solvent inlet, E. solution inlet, F,G. to waste)

The assembled cell is held tightly together with cap screws. The solvent and solution cavities are fitted with entrance and exit lines (1/16 inch i.d. x 1/32 inch o.d. SS) leading to the pressure transducers, to the solvent and solution inlets, and to waste. Thus the cell can be loaded and flushed without disassembly.

C. Membrane Osmometer

A diagram of the osmometer is shown in Figure 2-2. The solution and solvent sides of the cell are independently connected to separate pressure transducers (Omega Engineering, model PX300-1 KG-V, 0-1000 psig) via cyclohexane filled 1/16 inch x 1/32 inch lines and to a Setra model 204D high accuracy differential pressure gage (0 to $\pm$ 25 psid, $1x10^{-4}$ psi sensitivity) that measures the pressure difference between the transducers. A bypass valve disengages the pressure transducers from the differential gage (for safety) except when osmometry data are being recorded. Two 30 mL cyclohexane-filled reservoirs dampen the effect of thermal pressure fluctuations of the hydraulic fluid (cyclohexane) in the lines connecting the osmometry cell to the transducers. External pressures up to 6.0 MPa were simultaneously applied to solvent and solution-filled compartments in the cell via a cyclohexane-filled pressure generator (High Pressure Engineering, Erie PA, model 50-6-15). The cell and reservoir temperatures were monitored by platinum resistance thermometry, and the average temperature change was ~ 0.03 °/hour with net temperature increase of 0.8°/48 hours while the osmotic pressure was measured from 0.1 to 6.0 MPa applied pressure.

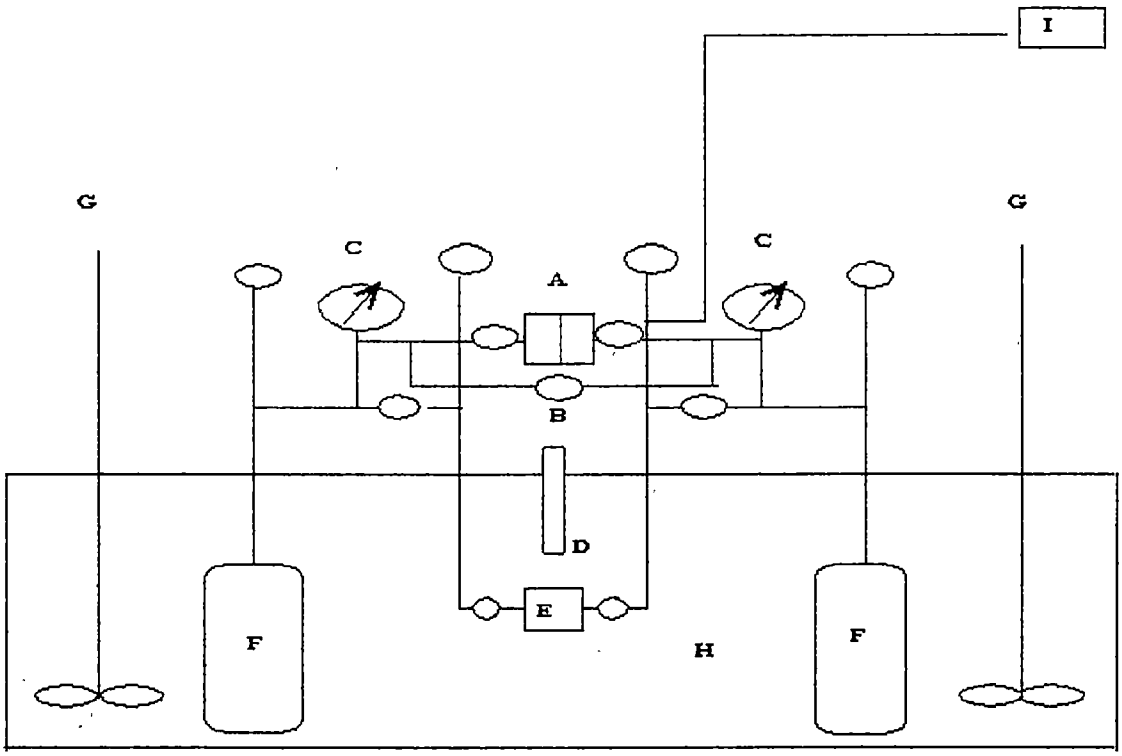

Figure 2-2. Membrane osmometer.

Key:
A. Differential pressure gauge
B. Bypass valve
C. Pressure transducers
D. Platinum resistance thermometer
E. Osmometry cell
F. Reservoirs
G. Stirrers
H. Water bath
I. Pressure generator

D. Typical Membrane Osmometry Experiment

To carry out an osmotic pressure measurement, the assembled cell was connected to the osmometer, loaded with solvent on both sides (Figure 2-1, p.20), and the bypass valve closed to measure the baseline at atmospheric pressure (external pressure = 0.1 Mpa). The solution compartment was then flushed and filled with solution (bypass open), the bypass valve closed, and differential gage pressure and temperature collected at regular intervals. In successive runs, pressure was simultaneously applied to solvent and solution in 1.0 MPa increments with the bypass valve open to prevent damage to the differential gage. The osmotic pressures (bypass closed) are the differences between the baseline value and the highest measured value at each increment of applied external pressure ($0.1 \leq P_{applied}/MPa \leq 6.0$). The QuickBasic program used for data collection is found in Appendix 1.

E. Materials and Sample Preparation (SLS)

Solvents (CH, MCH, toluene, decalin, and chloroform) were filtered through 0.1μm Whatman inorganic membrane filters before use. Solvents and polymers used are listed in Tables 2-2 and 2-3, respectively. Solution characteristics are listed in Table 2-4. SLS measurements were made with a Brookhaven Instruments Corp. package which includes a BI-200SM goniometer, BI-9025AT correlator, EMIB2FBK/RMI photomultiplier, Spectraphysics model 127 50-mW He-Ne laser, and a software package with Zimm and Debye plot functions. The light scattering set-up is shown in Figure 2-3.

Table 2-2

Solvents Used in SLS

Solvent	Source	Purity
toluene	Fisher Scientific	99.8%
cyclohexane	Aldrich Chemical Company, Inc.	99.5%, anhydrous
methylcyclohexane	Aldrich Chemical Company, Inc.	99%, anhydrous
50/50 *cis,trans*-decalin	Aldrich Chemical Company, Inc.	99%, anhydrous
chloroform	Fisher Scientific	certified ACS grade (0.75% C_2H_5OH)

Table 2-3

Polystyrene Samples Used in SLS

Polystyrene Molecular Weight x 10^{-3}(g/mol)	Polydispersity (M_w/M_n)	Source
900	1.06	Pressure Chemical
400	1.06	Pressure Chemical
417 *	unknown	*
228 *	unknown	*
90	1.04	Pressure Chemical
25	1.06	Pressure Chemical

*8-arm star polystyrenes contributed by Yuri Melnichenko, Oak Ridge National Laboratory, Oak Ridge, TN 37831

Table 2-4

Polystyrene Solutions Used in SLS

Solvent	Polystyrene Molecular Weight (g/mol x 10^{-3})	Concentration Range (mg/ml)	Pressure Range (MPa)	Temperature (°C)
toluene	90	2.00-16.00	0.1-35.0	22.0
toluene	400	0.26-1.63	0.1	22.0
toluene	417*	0.26-1.72	0.1	22.0
toluene	417* + 400	0.26-1.79	0.1	22.0
cyclohexane	25	3.91-12.00	0.1-30.0	25.0-45.0
cyclohexane	400	0.58-5.04	0.1-30.0	27.4
cyclohexane	400	0.20-1.06	0.1	23.0
cyclohexane	417*	0.20-1.00	0.1	22.0
cyclohexane	417* + 400	0.20-1.17	0.1	22.6
cyclohexane	900	0.40-2.20	0.1-0.30.0	29
methylcyclohexane	25	2.23-14.37	0.1-35.0	22.0
methylcyclohexane	400	0.13-0.25	0.1	58.0
methylcyclohexane	417*	0.13-0.28	0.1	58.0
methylcyclohexane	417* + 400	0.13-0.32	0.1	57.0-58.1
chloroform	90	2.00-15.30	0.1-35.0	22.0
decalin	90	1.93-15.50	0.1-35.0	22.0

*8-arm star polystyrene contributed by Yuri Melnichenko, Oak Ridge National Laboratory, Oak Ridge, TN 37831

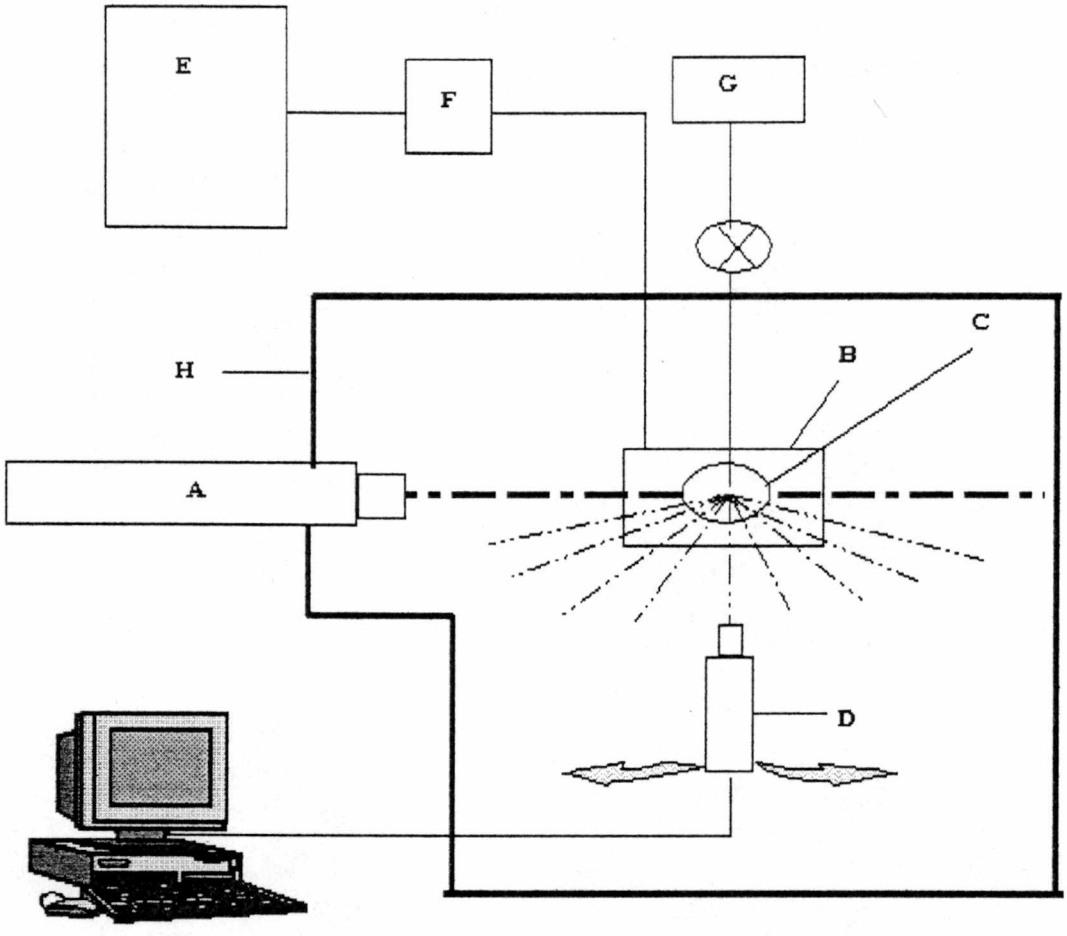

Figure 2-3. SLS experimental set-up.

Key:
A. Helium-neon laser (λ = 633.8 nm)
B. Toluene bath
C. Light scattering cell
D. Goniometer
E. Temperature bath
F. Filter
G. Pressure generator
H. Black box housing

Light scattering intensities of dilute polystyrene solutions at atmospheric pressure were collected for ($35 \leq \theta \leq 135$). Second virial coefficients were obtained from Zimm analysis of these data and compared to literature values to ensure proper working order of the Brookhaven instrument. Moderate pressure light scattering measurements (0.1-35.0 MPa) were then conducted at $\theta = 90$ to obtain A_2 from Debye analysis. Scattering cell design, discussed below, constrains Debye measurements to $\theta = 90$.

Solvent refractive indexes (n_0) and solution refractive index increments (dn/dc) at ambient temperature were obtained from Brandrup[9] and used to calculate second virial coefficients from Zimm and Debye analysis of light scattering intensity data. For A_2 measurements of PS/CH at 41 and 45 °C, the refractive index of cyclohexane and refractive increment of polystyrene in cyclohexane were obtained from Heller.[33]

F. SLS Cell

Light scattering intensity data were collected from solutions contained in glass vials at atmospheric pressure. From ($0.1 < P_{applied}/MPa \leq 35.0$ MPa) light scattering measurements were carried out in a stainless steel cell whose design and size (33 mm height, 27 mm diameter) are compatible with the Brookhaven instrument. A diagram of the cell is shown in Figure 2-4. The cell body encloses a "T" shaped optical path with 2.5 mm long "arms". Each arm terminates in a flat sapphire window[34] such that the laser beam passes through the solution compartment and scattering intensity is monitored by

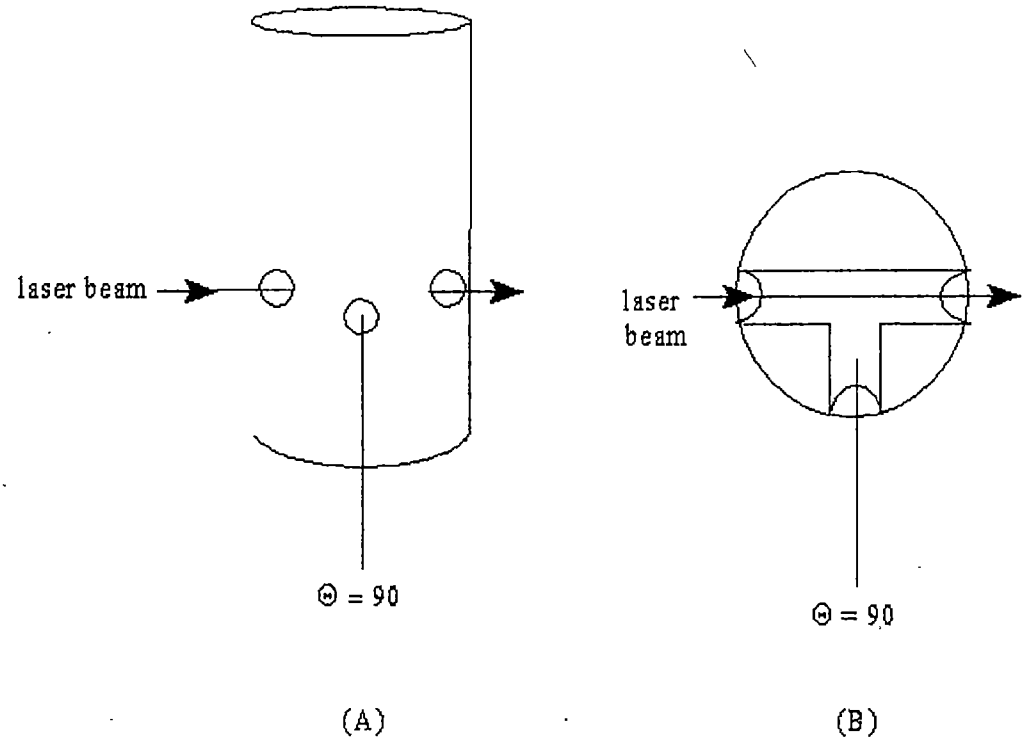

Figure 2-4. SLS cell. (A) cell body (B) "T"-shaped optical path

the detector at $\theta = 90$. Each window (6.3 mm diameter x 3.2 mm thickness) is seated on a 6.25 mm polished shoulder and gasketed on either side with annealed, polished soft copper gaskets. This assembly is held in place with hardened steel cap screws torqued to approximately 30 ft-lbs.[28]

The cell is centered in a toluene-filled vat during the experiment. Toluene, which has a refractive index close to that of glass, is circulated through a 0.2 μm filter (Cole-Parmer Instrument Company) to remove dust and a temperature-controlled bath (Hart Scientific model 704, $\pm$ 0.001°C) before it is returned to the vat. Temperature is measured with a 100 Ω RTD platinum resistance thermometer (Omega Engineering) located in a 1/8 inch diameter well in the top of the cell (calibrating equation: t/C = -263.294 + 2.625(Ω)). Average temperature stability during measurements as well as run-to-run temperature reproducibility is ~0.1°C.[28]

Sample enters and leaves through a 1/16 inch path drilled into the center of the cell which is connected to 1/16 inch stainless entrance and exit lines. These lines are connected to 1/16 inch valves which lead either to the pressure generator filled with acetone (HiP pressure generator, model 50-5.75-30) by way of a solution buffer volume or to waste. The buffer volume is large enough to allow for up to 10% compression of the solution without solvent/hydraulic fluid mixing. This design allows for the cell to be loaded and flushed without removing it from the vat. Pressure was monitored with a 0.01% precision electrical transducer (Precise Sensors, Inc., Monrovia, CA, model 6550).[35]

G. Cloud Point Measurements

Cloud point temperatures of linear polystyrenes and 8-arm star polystyrenes (Table 2-5) dissolved in CH and in MCH were measured by platinum resistance thermometry.[36] Samples were immersed in a water bath whose temperature was slowly lowered or raised until the solution became slightly turbid upon visual inspection. The temperature at the very onset of turbidity was taken as the cloud point. Lowering the temperature an additional tenth of a degree (approximately) induced pronounced clouding in the bulk solution.

Table 2-5

Solutions Used in Cloud Point Measurements

Solvent	Polystyrene Molecular Weight (g/mol x 10^{-3})	Concentration Range (mg/ml)
cyclohexane	*228	0.40 - 141.00
cyclohexane	*417	0.32 - 118.00
methylcyclohexane	17.5	8.30 - 316.70
methylcyclohexane	65	5.00 - 272.00
methylcyclohexane	*228	0.10 - 128.00
methylcyclohexane	400	2.00 - 299.00
methylcyclohexane	*417	0.13 - 42.00
methylcyclohexane	900	2.50 - 106.00

*8-arm star polystyrene contributed by Yuri Melnichenko, Oak Ridge National Laboratory, Oak Ridge, TN 37831

Chapter 3

Results

A. Membrane Osmometry

Plots of differential gage pressure against time for 1% (w/w) polystyrene 100,000 g/mol (PS 100k) in toluene are shown in Figure 3-1. After each incremental increase of applied external pressure, the differential gage pressure rises to its equilibrium value, and the system maintains that pressure for many tens of minutes. At atmospheric pressure, the differential gage pressure reaches its equilibrium value after approximately 300 minutes (time axis in Figure 3-1 has been truncated for presentation purposes). The system then fluctuates ($\pm$ 5%) about the equilibrium position for several hours. (The osmotic pressure is the difference between the baseline and the maximum differential gage pressure.) From a few other groups' membrane osmometry work,[37-40] we estimate an average error in osmotic pressure measurements to be on the order of 1-10% At higher externally-applied pressures (2.0 - 6.0 MPa) and for more concentrated solutions (discussed later), however, the amplitude of this fluctuation is much smaller ($\pm$ 1%).

Flory and Daoust[37] also observed fluctuations in osmotic pressures of polystyrene solutions during the first two to three hours of measurement with cellophane membranes, and they attributed these fluctuations to a membrane-distortion effect. Bawn, Freeman and Kamaliddin[41] observed that "new" cellophane membranes (those that had never been in contact with solution) used to measure osmotic pressures of polystyrene solutions gave lower-than-expected values of Π. After the membrane had been in contact with solution

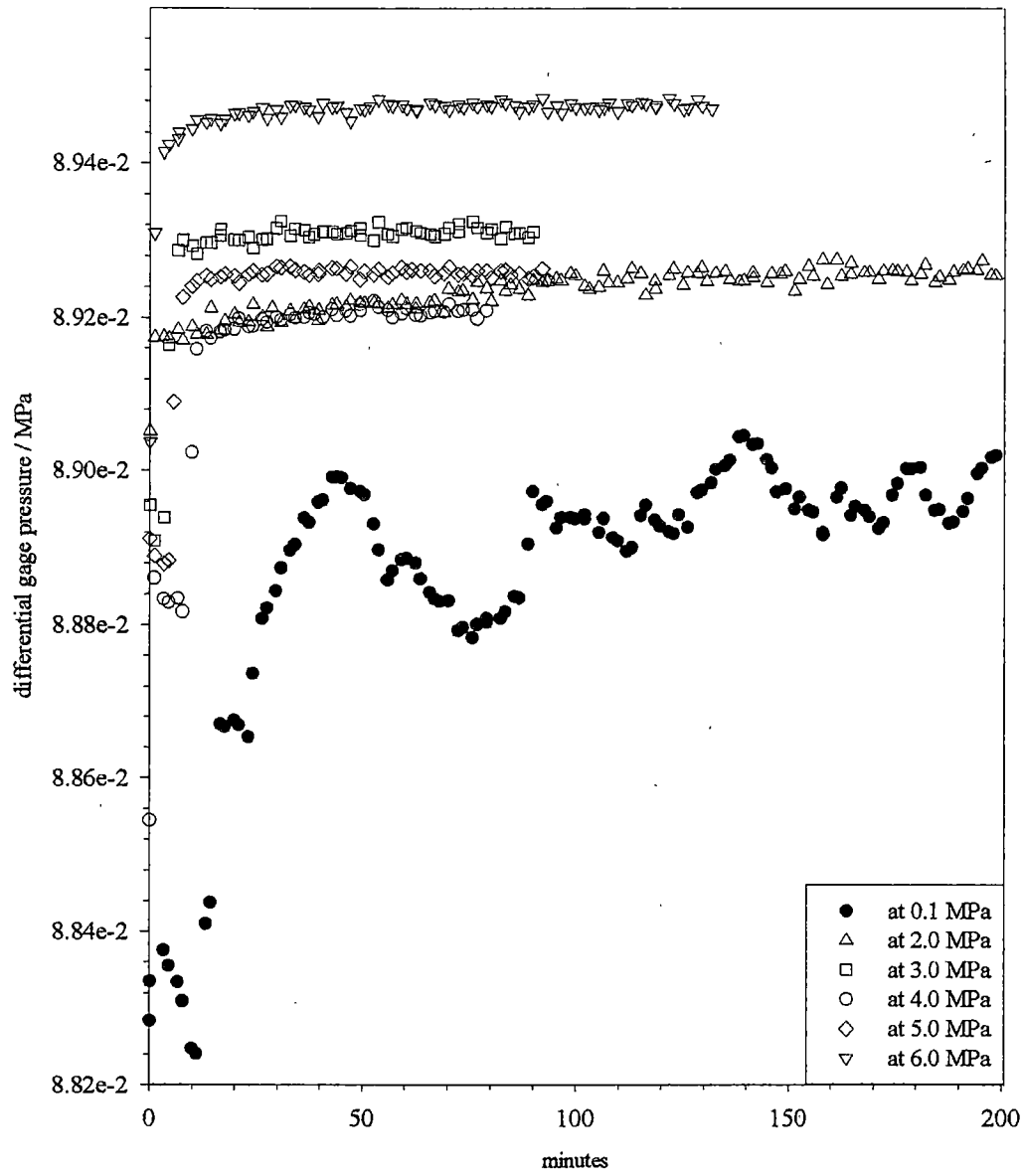

Figure 3-1. Developing osmotic pressure of 1% (w/w) PS 100k in toluene as a function of time and applied pressure.

for some time (the time period was not specified) and effectively "conditioned" to the solution, reasonable values of osmotic pressure were obtained.

In this work, with the first application of externally-applied pressure (1.0 MPa), the differential pressure decreases rather sharply as soon as the bypass valve is closed, then rebounds over the course of several hours to close to the original value recorded at atmospheric pressure. This behavior, consistently observed from membrane to membrane and solution to solution, is possibly due to a distortion of the membrane pores with externally-applied pressure. Sourirajan[42]discussed pore distortion in cellulose acetate membranes used in reverse osmosis experiments with $NaCl_{(aq)}$. The amount of NaCl removed from solution increased as operating pressure on the solution side of the membrane increased up to ~10 MPa, and he suggested this effect was in part attributable to a decrease in the average membrane pore size with increased operating pressure.

With successive applications of pressure (2.0-6.0 MPa), equilibrium is attained within approximately 30 minutes and sustained for tens of minutes, with fluctuations about the average on the order of 1%. In our experience, after 6.0 MPa of external pressure has been applied to the system, the membrane becomes unusable: If such a membrane is re-used to measure osmotic pressure at an externally-applied pressure equal to atmospheric pressure, no osmotic pressure develops.

Osmotic pressure measurements made in the semidilute region (3 and 5% (w/w) PS 100k/toluene; Figures 3-2 and 3-3, respectively) show an increasing tendency for the solute to leak across the membrane into the solvent compartment as applied pressure increases. One explanation is that increasing the externally-applied pressure on the system,

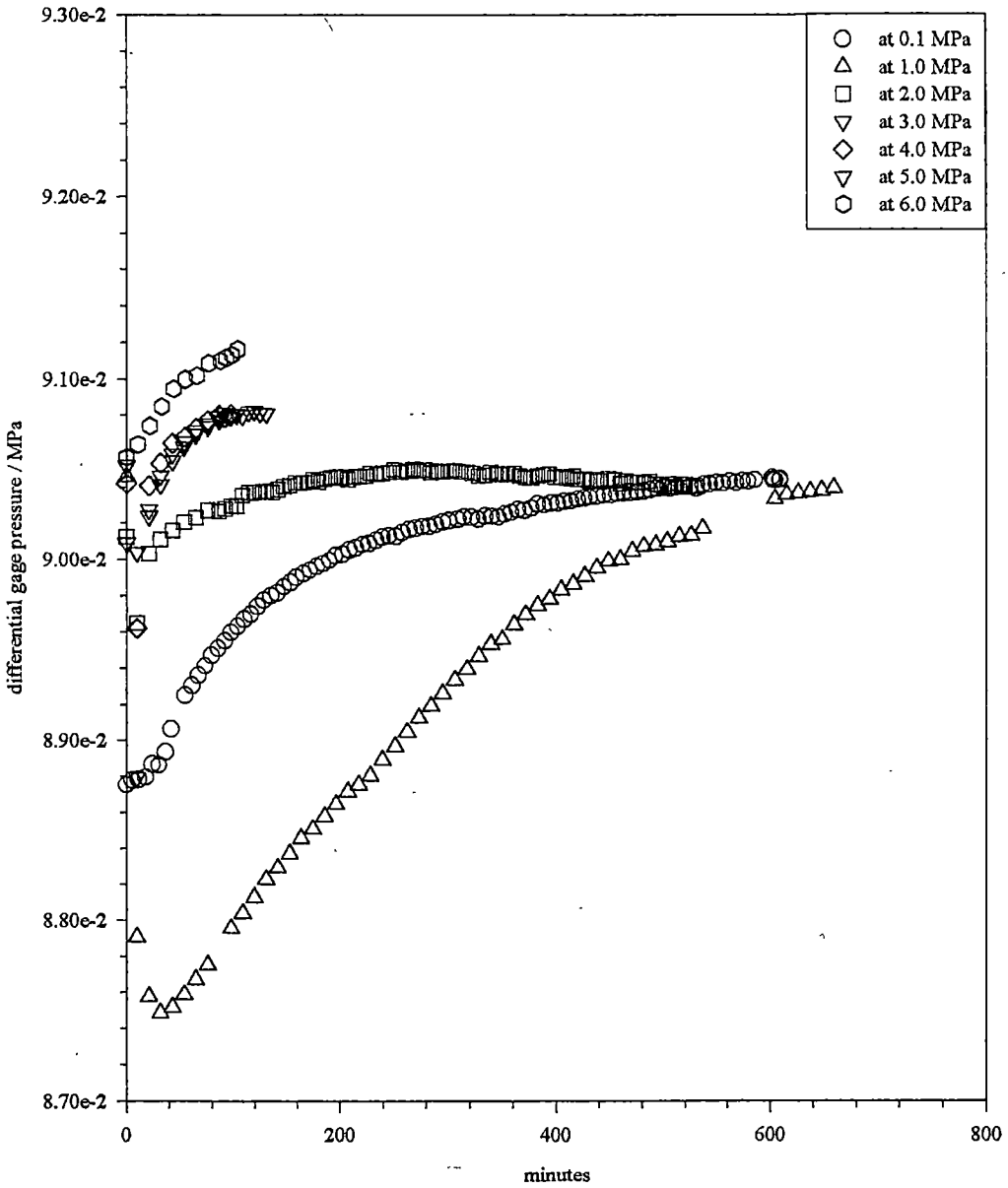

Figure 3-2. Developing osmotic pressure of 3% (w/w) PS 100k in toluene as a function of time and applied pressure.

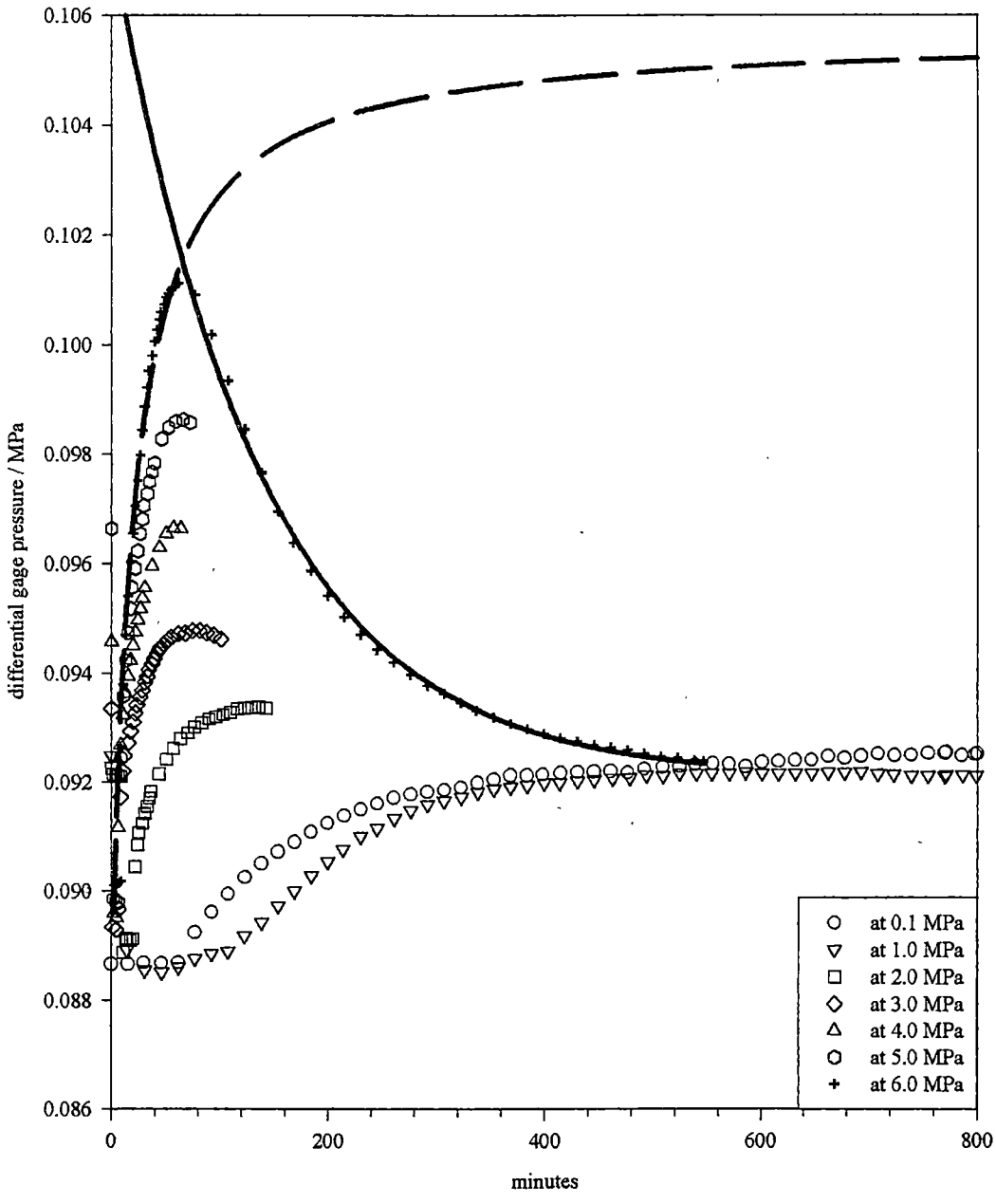

Figure 3-3. Developing osmotic pressure of 5% (w/w) PS 100k in toluene as a function of time and applied pressure.

which increases the pressure on the solution and solvent sides of the membrane, enlarges pores and allows polymer to cross the membrane into the pure solvent compartment. This effect is most clearly seen in (but certainly not limited to) the 6.0 MPa applied pressure curve of the 5% PS 100k/toluene solution in Figure 3-3, p. 37. If the membrane were completely impervious to polymer, the osmotic pressure would reach a maximum sustained value due to passage of solvent across the membrane. This situation is represented by the heavy, dashed line of the form $y = a(1-e^{-bx})$. However, when polymer crosses the membrane, the *measured* osmotic pressure (the difference between the baseline value and the highest differential gage value) is a function of the developing osmotic pressure (heavy, dashed line) and the leak rate of polymer across the membrane. The polymer leak-rate curve is represented by the heavy solid line and is of the form $y = y_0 + ae^{-bx}$. As a result, curve maxima at higher applied pressures are not equilibrium values, and 3 and 5% (w/w) PS/toluene data will not be compared to light scattering results reported in Chapter 3 of this work.

B. Pressure Coefficient of the Second Virial Coefficient from Membrane Osmometry

The virial expansion of osmotic pressure in terms of solute concentration may be truncated after the second virial term when measurements are carried out in dilute solution:[25]

$$\Pi = (RTc)\left(\frac{1}{M_n} + A_2c + \ldots\right) \qquad (3\text{-}1)$$

Concentration may be replaced by mass of solute(m_{II})/volume of solvent(V_I) to give

$$(\Pi) = \left(\frac{RTm_{II}}{M_n V_I}\right) + \left(\frac{RTA_2 m_{II}^2}{V_I^2}\right) . \qquad (3\text{-}2)$$

After partial differentiation with respect to pressure, the pressure coefficient of the osmotic pressure, $\frac{\partial \Pi}{\partial P}$, is

$$\frac{\partial \Pi}{\partial P} = \left[\left(\frac{RTm_{II}}{M_n}\right)(V_I)\left(\frac{\partial}{\partial P}\right)\left(\frac{1}{V_I}\right) + (RTm_{II}^2)\left(\frac{\partial}{\partial P}\right)\left(\frac{A_2}{V_I^2}\right)\right] \qquad (3\text{-}3)$$

which may be rewritten

$$\frac{\partial \Pi}{\partial P} = \left[\left(\frac{RTm_{II}}{M_n}\right)\left(\frac{-\partial V_I}{\partial P}\right)\left(\frac{1}{V_I}\right) + (RTm_{II}^2)\left(\frac{\partial}{\partial P}\right)\left\{\left(\frac{A_2}{V_I}\right)\left(\frac{1}{V_I}\right)\right\}\right] . \qquad (3\text{-}4)$$

Introducing the isothermal compressibility of the solvent $\left\{(\kappa) = \left[-\left(\frac{1}{V_I}\right)\left(\frac{dV_I}{dP}\right)\right]\right\}$,

$$\frac{\partial \Pi}{\partial P} = \left\{\frac{RTm_{II}}{V_I}\left[\left(\frac{\kappa}{M_n}\right) + \left(\frac{m_{II}}{V_I}\right)\left(\frac{\partial A_2}{\partial P} + \frac{2m\kappa A_2}{V_I}\right)\right]\right\} . \qquad (3\text{-}5)$$

Therefore, the pressure coefficient of the second virial coefficient, $\frac{\partial A_2}{\partial P}$, is

$$\left[\frac{\partial A_2}{\partial P} = \left\{\frac{V_I}{m_{II}}\left[\left(\frac{\partial \Pi}{\partial P}\right)\left(\frac{V_I}{RTm_{II}}\right) - \left(\frac{\kappa}{M_n}\right) - 2\left(\frac{m_{II}\kappa A_2}{V_I}\right)\right]\right\}\right] . \qquad (3\text{-}6)$$

The slope ($\partial\Pi/\partial P$ = 1.2 (±0.8) x 10^{-5} MPa/MPa applied) obtained from Figure 3-4 gives $\partial A_2/\partial P$ = 6 (±4) x 10^{-5} cm^3 mol g^{-2} MPa^{-1}, which is in reasonable agreement with static light scattering results (to be) presented in this work over the applied pressure range (0.1 to 6.0 MPa).

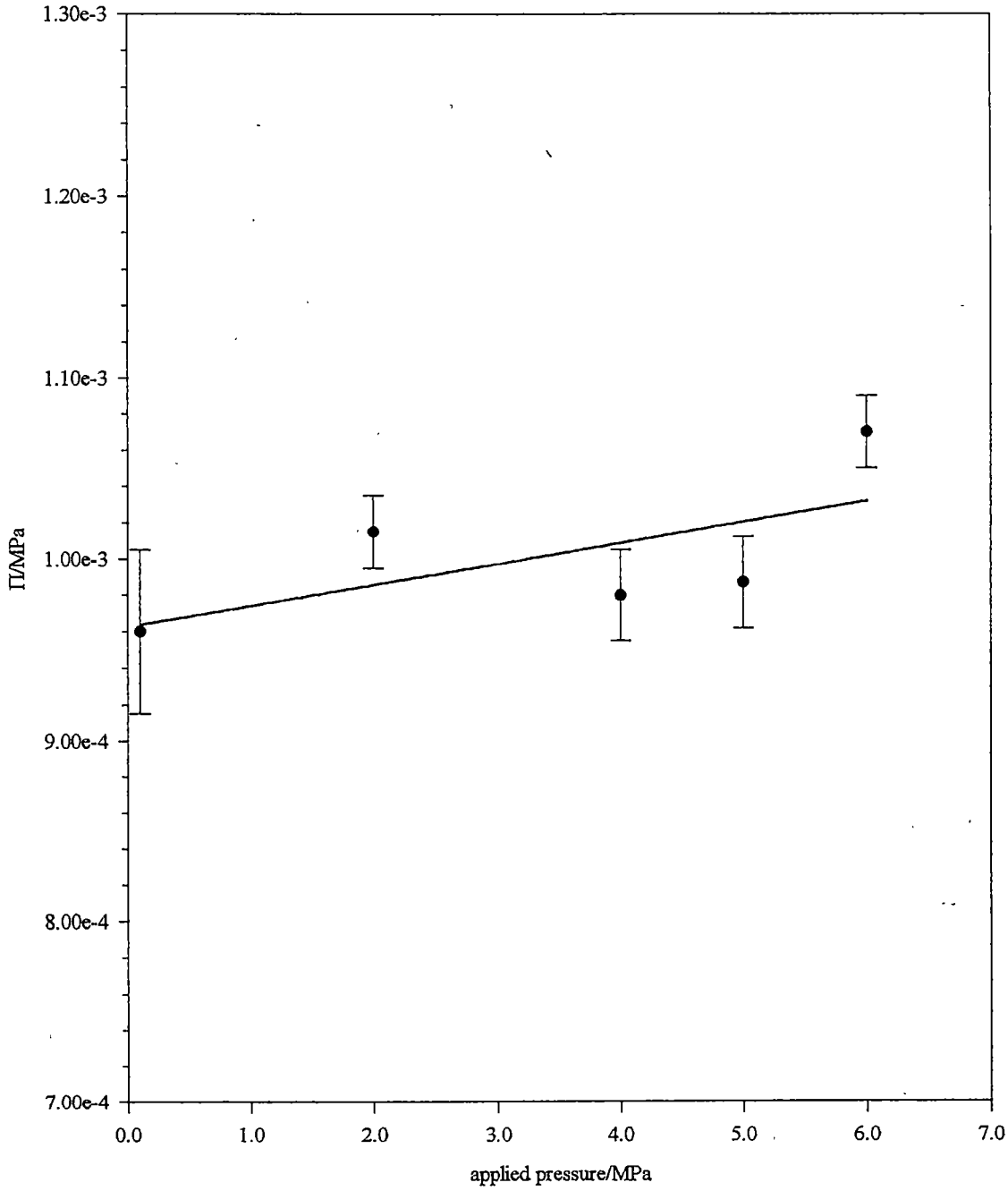

Figure 3-4. Osmotic pressure of 1% (w/w) PS 100k in toluene as a function of applied pressure.

The change in osmotic pressure with applied pressure is a very small effect and is difficult to measure to high precision; therefore, small uncertainties in $\partial\Pi/\partial P$ lead to relatively large uncertainties in $\partial A_2/\partial P$. The second virial pressure coefficient ($\partial A_2/\partial P$) of PS 100k in toluene, obtained from membrane osmometry, is in reasonable agreement with the SLS result to be discussed later{$dA_2/dP = 1.1\ (\pm 0.1) \times 10^{-5}$ cm^3 mol g^{-2} MPa^{-1} for ($0.1 \leq P_{applied}/MPa \leq 6.0$)}.

C. Pressure Coefficient of the Second Virial Coefficient from Static Light Scattering

Figure 3-5 shows the scattering intensity of PS 90k/toluene solutions over the applied pressure range 0.1 - 6.0 MPa. (Scattering intensity data for polystyrene in toluene, CH, MCH, decalin, and chloroform from 0.1 ~ 35.0 MPa applied pressure are located in Appendix 2.) Linear best-fit lines are applied to scattering data at each concentration, and the error in the slope of scattering intensity against applied pressure is propagated into the errors in A_2 and dA_2/dP.

SLS intensities were used to determine second virial coefficients at 0.1 MPa and their pressure dependences using Debye fits. Figure 3-6 shows the pressure dependence of A_2 for PS 90k/toluene for ($0.1 \leq P_{applied}/MPa \leq 6.0$) to be $1.0\ (\pm 0.1) \times 10^{-5}$ cm^3 mol g^{-2} MPa^{-1}. This result applies to scattering data collected over the concentration range 0.2 - 1.8 wt%. By comparison, dA_2/dP calculated from osmometry measurements on a 1 wt% solution is $6(\pm 4) \times 10^{-5}$ cm^3 mol g^{-2} MPa^{-1}.

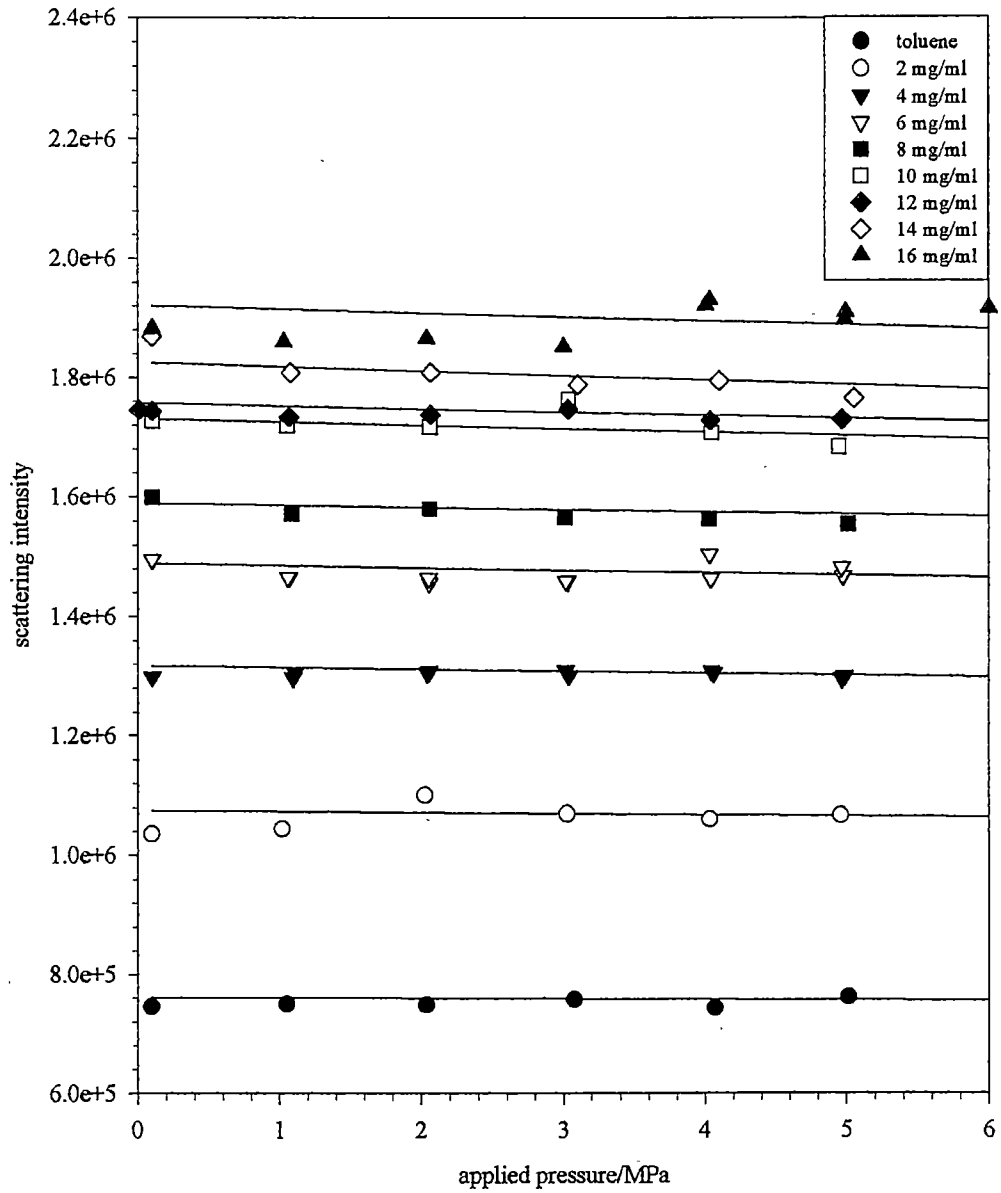

Figure 3-5. Scattering intensity of PS 90k in toluene as a function of applied pressure (0.1 to 6.0 MPa).

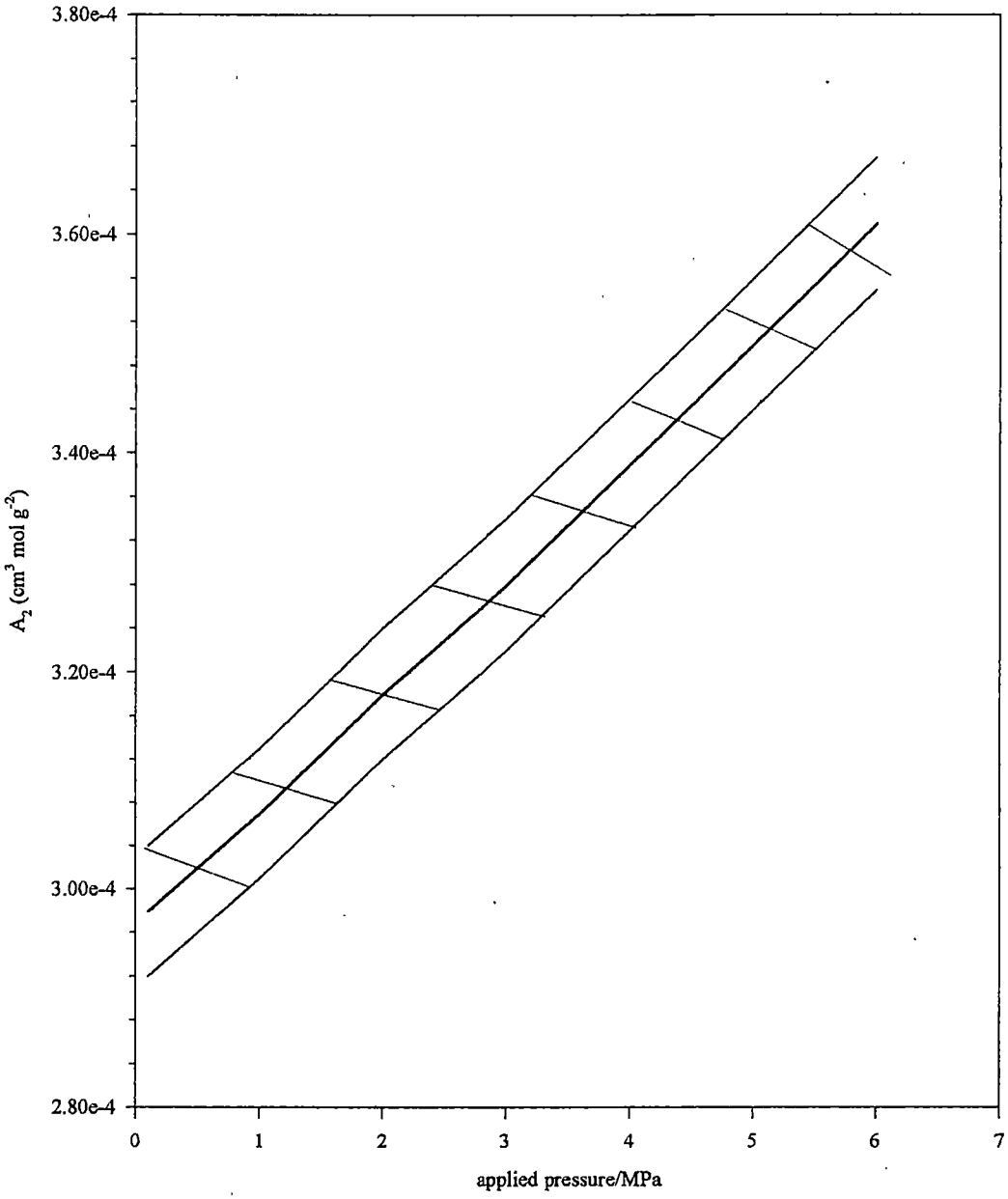

Figure 3-6. Second virial coefficient of PS 90k in toluene from 0.1 to 6.0 MPa.

Figure 3-7 shows the pressure dependence of A_2 for PS 90k in toluene, chloroform and decalin and PS 25k in MCH over the applied pressure range 0.1 - 35.0 MPa. The slopes are positive for PS in toluene, chloroform, and MCH, negative for PS in 50/50 *cis,trans*-decalin, and increase in magnitude in the order (decalin < chloroform < toluene < MCH). The error in the decalin pressure coefficient as a percentage of the overall pressure coefficient is significantly larger than in toluene, chloroform, and MCH. Polystyrene has a θ temperature of 12.3°C in *cis*-decalin and 21.4°C in *trans*-decalin, the poorer solvent;[14] therefore, a 50/50 mixture of isomers is expected to be a theta-to-poor solvent. Since methylcyclohexane is a poor solvent for polystyrene, both the molecular weight used and the solution concentration range studied were much lower than in decalin, chloroform, and toluene.

The pressure coefficient of PS 25k in CH was studied above and below $\theta_T = 34 - 35°C$[43-45](Figure 3-8). dA_2/dP is negative at 22 and 41°C and positive at 45 °C, with the trend in slopes 22°C < 41°C < 45 °C. In higher molecular weight systems near 30 °C, the sign of dA_2/dP changes from positive to negative for PS 400k/CH and PS 900k/CH, respectively (Figure 3-9).

Second virial coefficients for polystyrene in all solvents at atmospheric pressure (0.1 MPa), along with their pressure coefficients, are reported in Table 3-1 and compared where possible with literature data. For almost all solutions, A_2 was first calculated from Zimm plots at 0.1 MPa and compared to literature values to confirm that results were within expected ranges. A_2 values obtained from Debye plots at θ = 90 were then used to

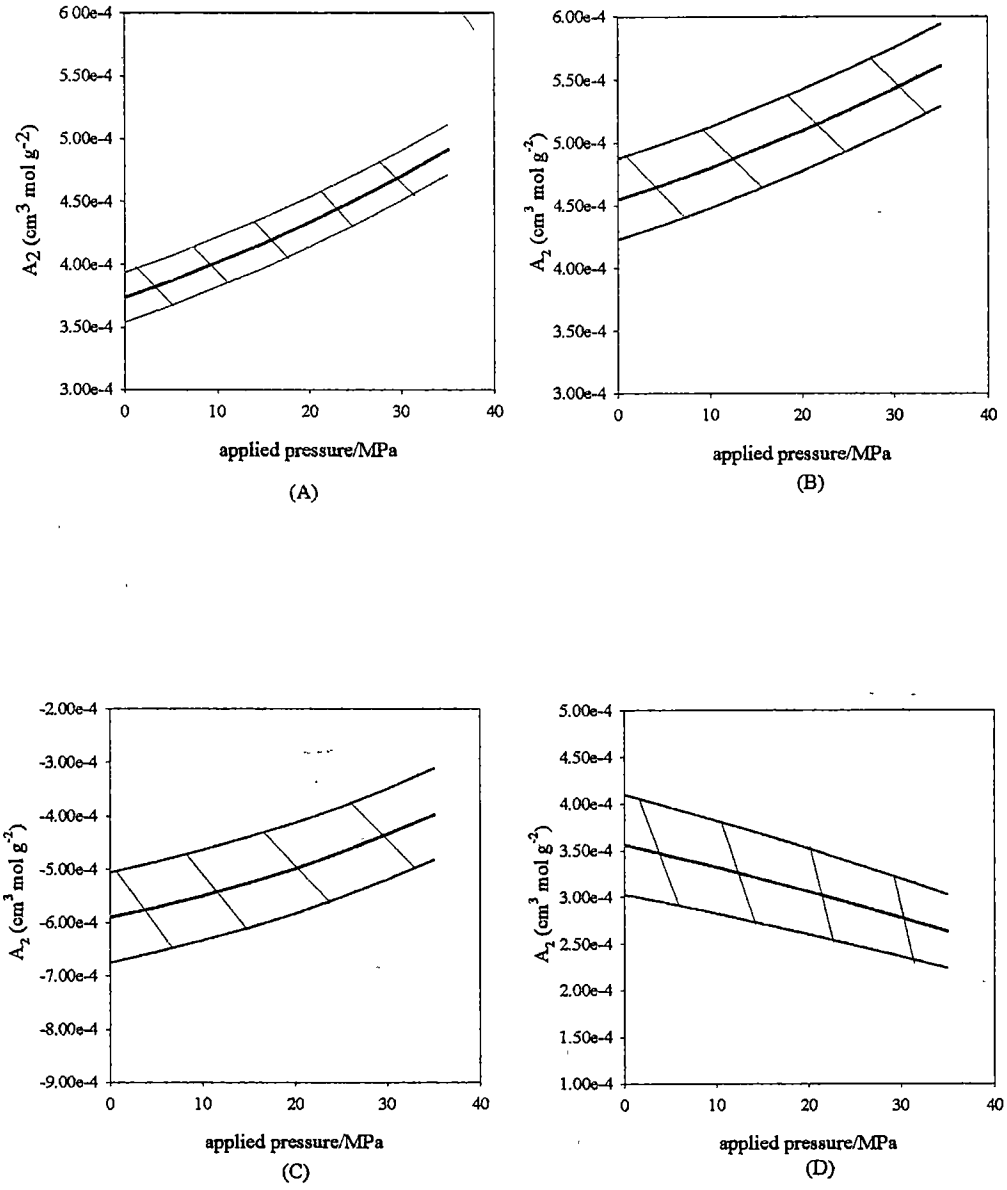

Figure 3-7. Second virial coefficients of polystyrene in various organic solvents near 25°C as a function of applied pressure. (A) PS 90k/toluene, (B) PS 90k/chloroform, (C) PS 25k/MCH, and (D) PS 90k/*cis,trans*-decalin

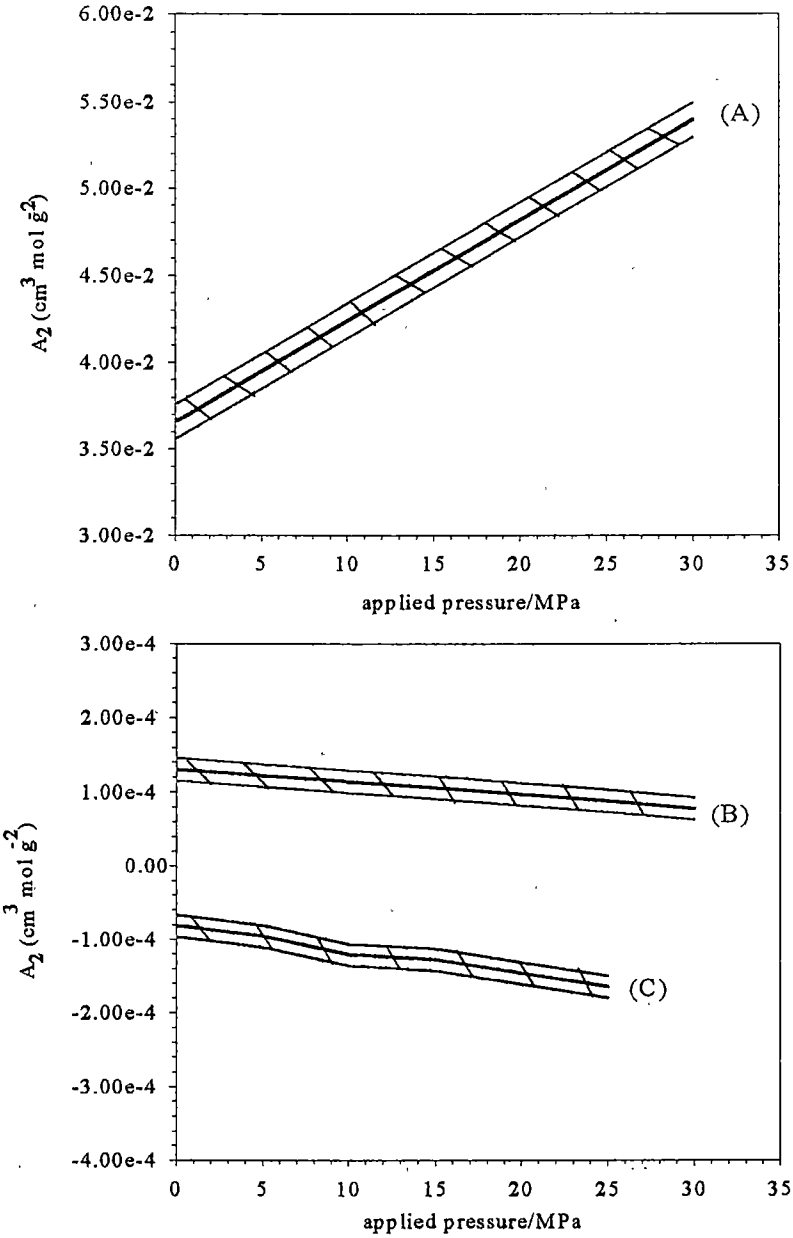

Figure 3-8. Second virial coefficient of PS 25k in CH from 22 - 45°C as a function of applied pressure. (A) PS 25k/CH at 45°C, (B) PS 25k/CH at 41°C, and (C) PS 25k/CH at 22°C

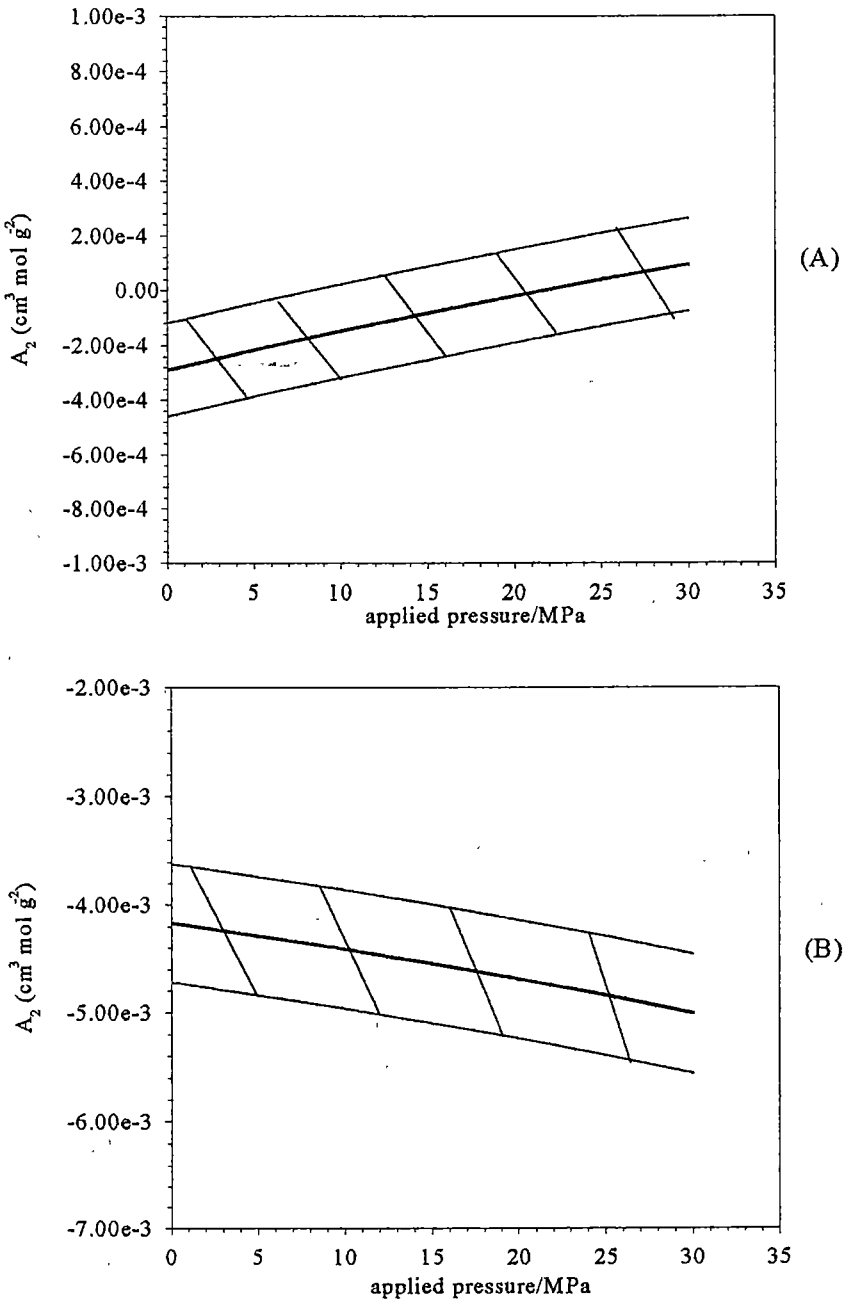

Figure 3-9. Second virial coefficients of PS 400k and PS 900k in CH near 30°C as a function of applied pressure. (A) PS 400k/CH at 27°C, and (B) PS 900k/CH at 29°C

Table 3-1

Second Virial Coefficients and Pressure Coefficients of Second Virial

Coefficients of Polystyrene Dissolved in Various Organic Solvents

Solution	Temperature/°C	A_2 (cm^3 mol g^{-2}) from Zimm Plot (θ = 35-135°)	A_2 (cm^3 mol g^{-2}) (literature)	A_2 (cm^3 mol g^{-2}) from Debye Plot (θ = 90°)	dA_2/dP (cm^3 mol g^{-2} MPa^{-1}), 0.1-35 MPa Applied
PS 100k/toluene	25				6.3×10^{-5} (osmometry; 0.1 - 6.0 MPa applied)
PS 90k/toluene	25	3.51×10^{-4}	3.3×10^{-4} (PS 100k, 25° C)[28]	2.98×10^{-4}	1.07×10^{-5} (0.1 to 6.0 MPa applied)
PS 90k/toluene	25	3.51×10^{-4}			3.37×10^{-6}
PS 90k/chloroform	25	8.03×10^{-4}	8.0×10^{-4} (PS 372k, 20° C)[9]	4.55×10^{-4}	3.04×10^{-6}
PS 90k/50-50 *cis-trans* decalin	25	4.74×10^{-5}	0.19×10^{-4} to -0.01×10^{-4} (PS 1800k, 25° C)[9]	2.02×10^{-4}	-2.57×10^{-6}
PS 25k/MCH	22	-1.21×10^{-3}	-4.5×10^{-4} (PS 17.5k, 22° C)[28]	-5.90×10^{-4}	5.50×10^{-6}
PS 25k/CH	22	-8.03×10^{-4}	-0.410×10^{-4} (PS 68.7k, 23° C)[9]	-2.07×10^{-3}	-3.28×10^{-6} *

Table 3-1 continued

Solution	Temperature/°C	A_2 (cm^3 mol g^{-2}) from Zimm Plot (θ = 35-135°)	A_2 (cm^3 mol g^{-2}) (literature)	A_2 (cm^3 mol g^{-2}) from Debye Plot (θ = 90°)	dA_2/dP (cm^3 mol g^{-2} MPa^{-1}), 0.1-35 MPa Applied
PS 25k/CH	41	-2.82×10^{-4}	0.634×10^{-4} (PS 50k, 40° C)[9]	8.79×10^{-5}	-1.70×10^{-6}
PS 25k/CH	45	-1.74×10^{-4}	0.79×10^{-4} to 0.87×10^{-4} (PS 100k, 45°C)[9]	0.0366	5.81×10^{-4}
PS 400k/CH	27	-1.65×10^{-4}	-6.0×10^{-5} (PS 400k, 27° C)[28]	-2.89×10^{-4}	1.28×10^{-5}
PS 900k/CH	29	-1.03×10^{-4}	-0.37×10^{-4} to 0.258×10^{-4} (PS 1610k, 27 to 41.5° C)[9]	-4.19×10^{-3}	-2.79×10^{-5}

*0.1-30.0 MPa applied pressure

calculate the pressure coefficient, dA_2/dP.

D. Second Virial Cross Coefficients Between Linear and Star Polystyrenes

Second virial cross coefficients quantify the extent of linear-star PS interactions in dilute solution and can be obtained from second virial coefficients of solutions of varying linear-star ratios. Second virial coefficients of such PS mixtures in toluene, CH, and MCH were obtained from Zimm analysis of measured scattering intensities as a function of solution composition for ($35 \leq \theta \leq 135$). These data are reported in Table 3-2 and plotted in Figure 3-10 along with their fit to equation (3-7) (discussed below). Error bars represent the average error in A_2 calculated from the distribution of scattering intensity data for each family of solutions in a particular solvent.

Second virial coefficients and second virial cross coefficients reported in Table 3-3 were obtained by fitting SLS second virial coefficients in Table 3-2 to equation 3-7. The initial parameters used were (100% linear) PS $A_{2(L\text{-}L)}$, (100% star) PS $A_{2(S\text{-}S)}$, and $A_{2(L\text{-}S)} = (A_{2(L\text{-}L)} + A_{2(S\text{-}S)})/2$. The fitting equation is of the form[30]

$$f = (1\text{-}S)^2B + S^2C + 2S(1\text{-}S)D, \qquad (3\text{-}7)$$

in which S = weight fraction of 8-arm star PS 417k, $B = A_{2(L\text{-}L)}$, $C = A_{2(S\text{-}S)}$, and $D = A_{2(L\text{-}S)}$.

Table 3-2

Second Virial Coefficients of Linear and Star Polystyrene Solutions

Weight Fraction of 8-Arm Star PS 417k	A_2 ($\pm$ 1.0) (10^{-4} cm3 mol g^{-2}) in Toluene at 25°C	A_2 ($\pm$ 0.7) (10^{-4} cm^3 mol g^{-2}) in Cyclohexane at 25°C	A_2 ($\pm$ 2.0) (10^{-4} cm^3 mol g^{-2}) in Methylcyclohexane at 58.3°C	A_2 (10^{-4} cm^3 mol g^{-2}), literature[46]
0.00	2.59			
0.30	-1.17			
0.50	0.46			
0.71	-0.90			
1.00	0.33			3.5 $\pm$ 0.5 (8-arm star PS 391k/toluene at 31.2°C)
0.00		-3.09		
0.36		-2.95		
0.50		-3.17		
0.70		-3.32		
1.00		-3.26		0.79 $\pm$ 0.04 (8-arm star PS 391k/CH at 34.0°C)

Table 3-2 continued

Weight Fraction of 8-Arm Star PS 417k	A_2 ($\pm$ 1.0) (10^{-4} cm3 mol g^{-2}) in Toluene at 25°C	A_2 ($\pm$ 0.7) (10^{-4} cm^3 mol g^{-2}) in Cyclohexane at 25°C	A_2 ($\pm$ 2.0) (10^{-4} cm^3 mol g^{-2}) in Methylcyclohexane at 58.3°C	A_2 (10^{-4} cm^3 mol g^{-2}), literature[46]
0.00			-7.58	
0.30			-13.40	
0.50			-3.65	
0.67			-15.00	
1.00			-8.58	1.3 $\pm$ 0.4 (8-arm star PS 74k/MCH at 50.0°C)

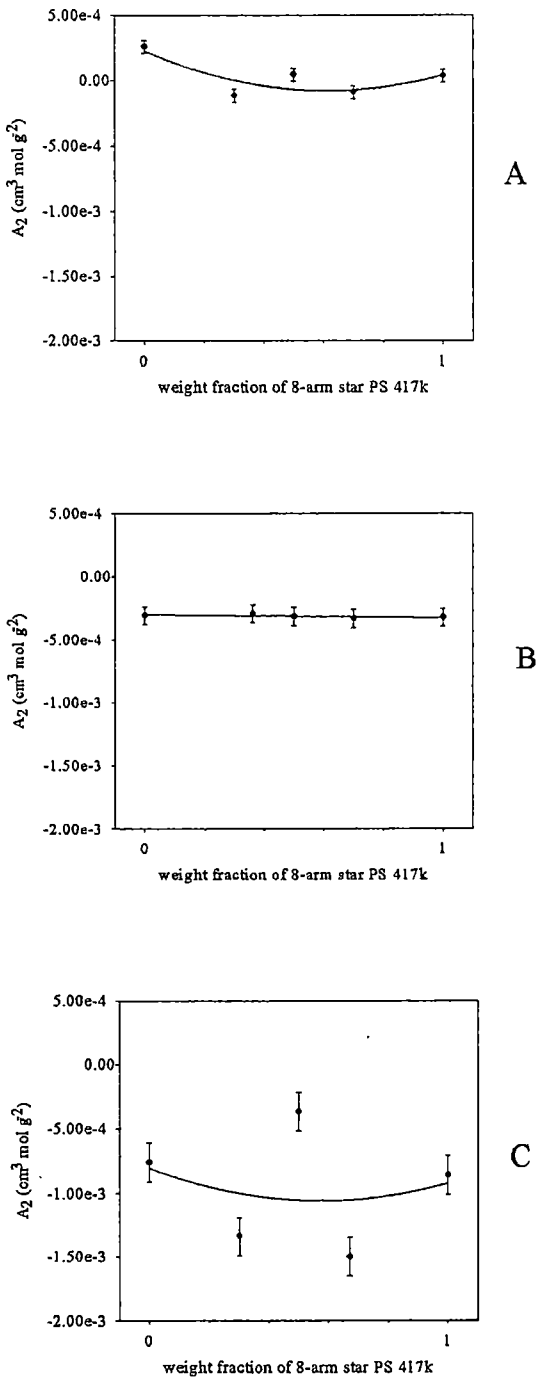

Figure 3-10. Second virial coefficients of linear PS 400k and 8-arm star PS 417k mixtures in (A) toluene, (B) CH, and (C) MCH.

Table 3-3

Initial and Fit Parameters to Determine Second Virial Cross Coefficients

Parameter	Toluene (25°C)	CH (25°C)	MCH (58°C)
$B_{initial}$ (cm^3 mol g^{-2})	2.59 ($\pm$ 1.0)x 10^{-4}	-3.09($\pm$ 0.7) x 10^{-4}	-7.58($\pm$ 2.0) x 10^{-4}
$C_{initial}$ (cm^3 mol g^{-2})	3.30($\pm$ 1.0) x 10^{-5}	-3.26($\pm$ 0.7) x 10^{-4}	-8.58($\pm$ 2.0) x 10^{-4}
$*D_{initial}$ (cm^3 mol g^{-2})	1.46 x 10^{-4}	-3.16 x 10^{-4}	-8.08 x 10^{-4}
B_{fit} (cm^3 mol g^{-2})	2.28($\pm$ 1.0) x 10^{-4}	-3.05($\pm$ 0.7) x 10^{-4}	-8.04($\pm$ 2.0) x 10^{-4}
C_{fit} (cm^3 mol g^{-2})	4.22($\pm$ 1.0) x 10^{-5}	-3.31($\pm$ 0.7) x 10^{-4}	-9.20($\pm$ 2.0) x 10^{-4}
D_{fit} (cm^3 mol g^{-2})	-2.71($\pm$ 1.9) x 10^{-4}	-3.09($\pm$ 0.2) x 10^{-4}	-1.24($\pm$ 1.0) x 10^{-3}

Key

$B = A_{2(L\text{-}L)}$

$C = A_{2(S\text{-}S)}$

$D = A_{2(L\text{-}S)}$

$$*D_{initial} = \frac{B_{initial} - C_{initial}}{2}$$

E. Cloud Points of Linear and Star Polystyrenes in Cyclohexane and Methylcyclohexane

Cloud point temperatures of linear ($17{,}500 \leq M \leq 900{,}000$ g/mol) and star (M = 228,000 and 417,000 g/mol) polystyrenes in CH and MCH were measured to study the effect of chain architecture on solubility. Cloud point measurements of star polystyrenes and nearly monodisperse linear polystyrenes in CH and MCH (Figures 3-11 and 3-12, respectively) show that star PS 417k is slightly more soluble than linear PS 400k in both solvents, but the difference in linear and star PS upper critical solution temperatures (UCST) is small ($UCST_{\text{linear PS}} - UCST_{\text{star PS}} = \Delta UCST \sim 3°$). (When polydispersity is low ($M_w/M_n \cong 1$), the difference between the upper critical solution temperature and the maximum temperature in the cloud point VS solution composition curve is very small, and cloud points can be substituted for critical solution temperatures without significant error.)

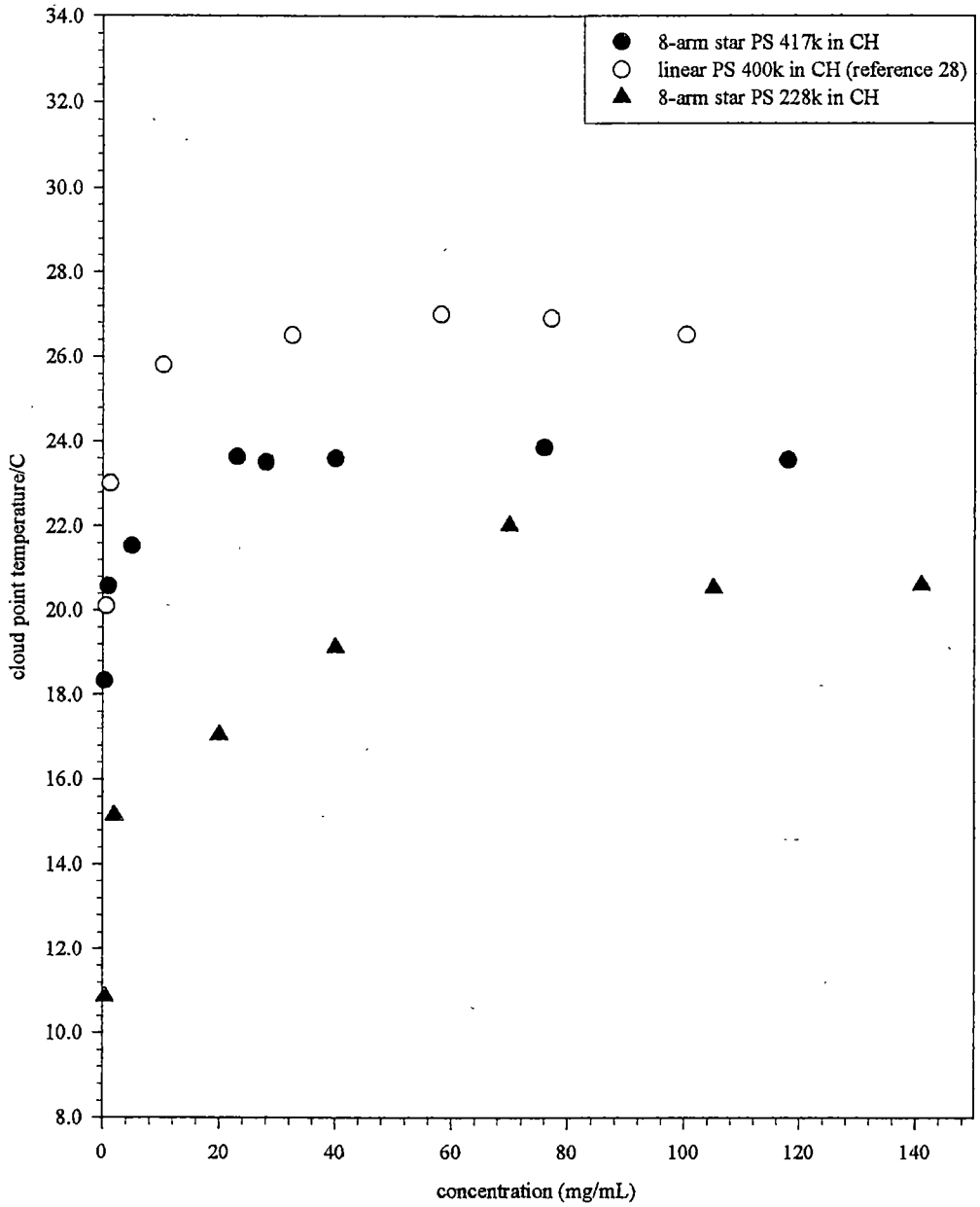

Figure 3-11. Cloud point temperatures of polystyrenes in CH.

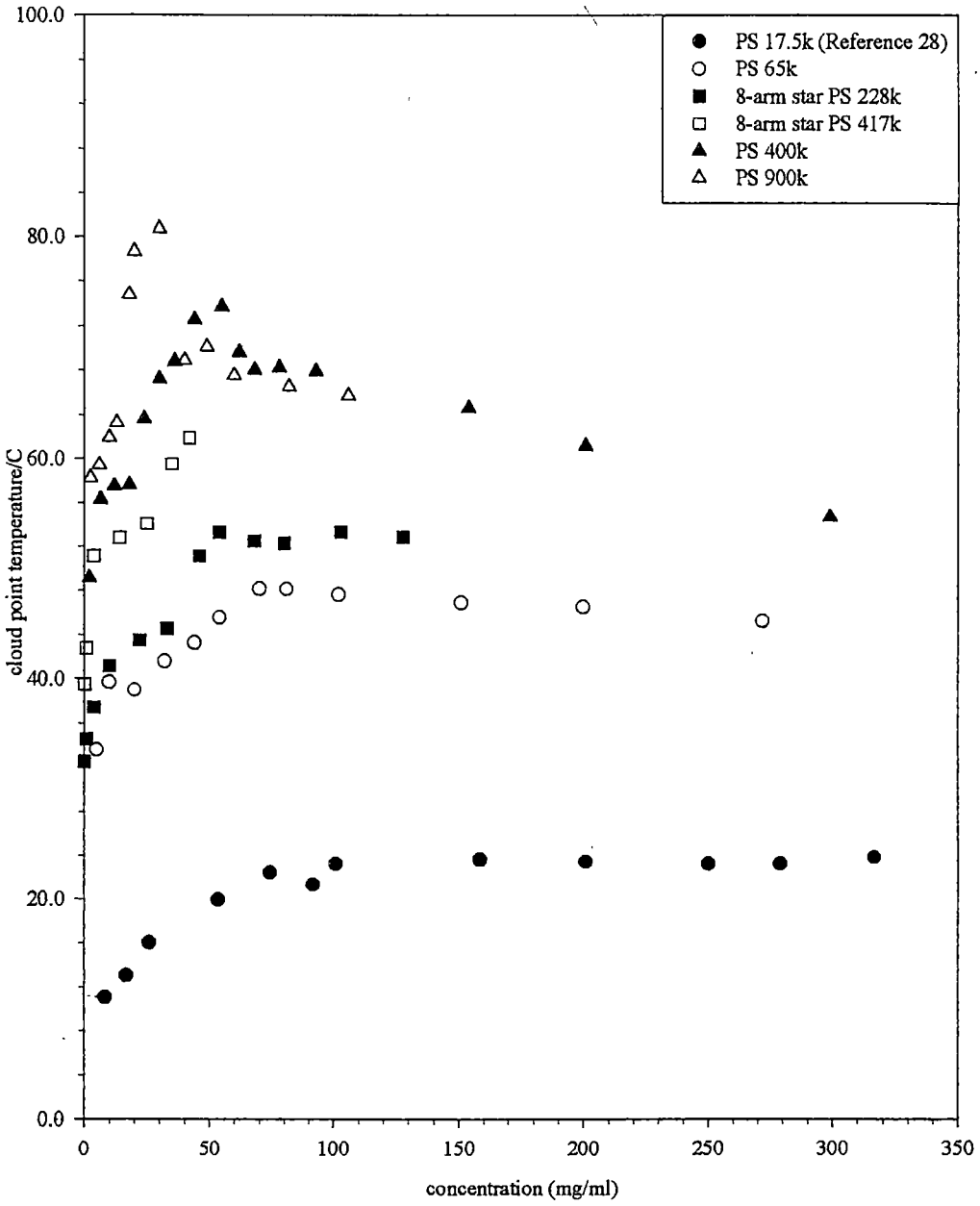

Figure 3-12. Cloud point temperatures of linear and 8-arm star polystyrenes in MCH.

Chapter 4

Discussion

Results presented in Chapter 3 show that the pressure coefficient of the second virial coefficient (dA_2/dP) can be used to determine how solvent quality changes with applied pressure. Solvent quality may either improve ($dA_2/dP > 0$), deteriorate ($dA_2/dP < 0$), or be unaffected ($dA_2/dP = 0$) by increases in applied external pressure. We have used membrane osmometry and static light scattering to obtain dA_2/dP and thus determine how solvent quality changes with applied pressure for linear polystyrene (PS) solutions. Others have used phase equilibria studies to determine how changes in the upper critical solution temperature (UCST) with applied pressure (dT_{UCST}/dP) affect solvent quality.

Polymer/θ-solvent solutions have separated upper and lower critical solution temperature (LCST) branches which enclose a homogeneous, one-phase region in [reciprocal critical temperature $(1/T)_{CR}$, reciprocal square root molecular weight $(1/M_w)^{1/2}$] space. As solvent quality improves from θ to good, the distance between UCST and LCST increases, as does the area of the one-phase region. If an increase in applied pressure increases the area of the one-phase region, $dT_{UCST}/dP > 0$ and $dT_{LCST}/dP < 0$. (Figure 1-1, p.5). Good solvent systems have larger one-phase solubility regions than θ solvent systems, and θ solvent systems have larger one-phase regions than poor solvent systems.[23, 24]

The pressure derivative of the upper critical solution temperature (dT_{UCST}/dP) is inversely related to dA_2/dP. Positive values of dT_{UCST}/dP correspond to negative values of dA_2/dP and vice versa. Various groups have reported (via dT_{UCST}/dP) that increasing

amounts of pressure applied to polymer solutions can improve solvent quality by transforming a θ solvent into a good solvent[47-51] and a poor solvent into a θ solvent.[52-53] However, while pressure does in many cases improve solvent quality, this behavior is by no means universal. There are cases in which solvent quality deteriorates with pressure. For example, Wells, de Loos, and Kleintjens[48] have reported from phase equilibrium studies of PS 22k/MCH that solvent quality improves (i.e. $dT_{UCST}/dP < 0$) when applied pressure is no greater than 40 MPa; however, above 50 MPa, solvent quality deteriorates ($dT_{UCST}/dP > 0$) . In the following discussion, we refer to dA_2/dP values reported in Chapter 3 of this work along with dT_{UCST}/dP data from the literature to determine how pressure applied to dilute PS solutions changes solvent quality.

We also comment on the interaction between polystyrenes of similar molecular weight but dissimilar architecture {e.g. linear (L) polystyrene and 8-arm star (S) polystyrene} in dilute solution. The extent of linear-star PS interaction was determined from the value of the SLS second virial *cross* coefficient ($A_{2(L-S)}$). The second virial cross coefficient ($A_{2(L-S)}$) is a combination of contributions from linear-linear PS interactions ($A_{2(L-L)}$), star-star PS interactions ($A_{2(S-S)}$), and linear-star PS interactions ($A_{2(L-S)}$).[17] We compare our SLS-obtained $A_{2(L-S)}$ data to membrane osmometry data reported by Striolo and Prausnitz[30] for linear-star PS systems.

We were interested to know how solubilities of linear and star polystyrenes differ from one another and how those differences affect $A_{2(L-S)}$. If the linear polymer is more soluble in a particular solvent than the star polymer (or vice versa), is the solubility difference (| linear solubility - star solubility |) large enough to affect $A_{2(L-S)}$ significantly?

To answer this question, we measured cloud points of linear polystyrenes and 8-arm star polystyrenes in CH and in MCH. (Solutions were composed of *either* a linear PS *or* a star PS dissolved in a single solvent.) The cloud point is the temperature at which precipitation first occurs and can be used as an indicator of polymer solubility in a particular solvent.

Cloud point temperatures were easy to obtain— at the first sign of turbidity, the temperature of the solution was measured with a platinum resistance thermometer. Osmotic pressure measurements were considerably more difficult to make, especially as applied pressure increased. In membrane osmometry, the membrane is the most important component in the experiment. It must have pores that are large enough to allow solvent to diffuse through but small enough to stop polymer molecules from doing the same. It must not be dissolved by, shrink in, or swell in solvents of interest, and it must be conditioned properly before use, not be allowed to dry out, and not torn or perforated during cell assembly and filling. It must be rugged and durable, able to function properly at pressures in excess of atmospheric, and the pores must not become distorted or clogged by polymer with use.

The cellulose acetate membranes used in our membrane osmometry experiments met these requirements and functioned well with dilute PS/toluene solutions. At applied pressure = atmospheric pressure, we measured the osmotic pressure of 1% (w/w) PS 100k/toluene to ± 5%. At higher applied pressures (2.0 - 6.0 MPa), the uncertainty in the osmotic pressure is estimated to be ± 1%. These uncertainties are commensurate with those reported by others [37-40] who report osmotic pressures (at applied external pressure = atmospheric pressure) to ~1-10%.

In θ and poor solvent systems, we encountered problems with the membrane. With osmotic pressure measurements on 5% (w/w) PS100k/CH (θ solvent), 3%(w/w) PS 100k/MCH (poor solvent), and 3% PS45k/butyl acetate (poor solvent), we discovered that (a) the membrane clogged immediately (i.e. at 0.1 MPa) or with successive applications of pressure or (b) the trend in the measured osmotic pressure as a function of applied external pressure was erratic, with no clearly emergent pattern over the applied pressure range. Therefore, osmotic pressure measurements in CH, MCH, and butyl acetate are not included in this work.

Static light scattering measurements were easier to make than osmotic pressure measurements. Removing dust particles from solvents and solutions was the most difficult part of scattering intensity measurements. Compared to the size of polymer molecules in solution, dust particles are large and preferentially scatter light to small angles.[54] Dust can effectively obscure light scattered by the solution; therefore, considerable effort was devoted to filtering solvents used in solution preparation.

It is obvious why there have so few studies published on the effect of pressure on second virial coefficients. The pressure effect (dA_2/dP) is very small and difficult to measure with accuracy and precision even when osmometry and light scattering cells and instrumentation have been carefully designed to function reliably at applied pressures in excess of atmospheric. Data listed in Chapter 3 were gathered with considerable attention to experimental design and protocol, and the light scattering and membrane osmometry results discussed below are, in most cases, of equal or better precision than data reported in the literature.

A. Pressure Coefficient of the Second Virial Coefficient of Polystyrene in Organic Solvents

Solvent quality in polymer solutions (one polymer + one solvent) is influenced by complex interactions among variables such as pressure, temperature, polymer molecular weight, and polymer concentration. In some systems, solvent quality is sensitive even to small changes in one or more of these variables. After reviewing the literature, we found very little work had been done on polystyrene solutions under pressure. Therefore, the primary goal of this project was to determine how pressure changes solvent quality in dilute polystyrene solutions. We have accomplished this task using membrane osmometry (MO) and static light scattering on a variety of PS/organic solvent systems. To our knowledge, only one other group[16] has used membrane osmometry to study the thermodynamic behavior of a polymer solution under pressure.

We have also studied effects of temperature and molecular weight on one system—PS/CH. dA_2/dP, the pressure coefficient of the second virial coefficient (A_2) obtained from MO and SLS, was the criterion used to assign solvent quality. When $dA_2/dP > 0$, solvent quality improves with applied pressure, and when $dA_2/dP < 0$, solvent quality deteriorates with pressure.

Results obtained at room temperature show solvent quality improves with applied pressure in the good (PS/toluene, PS/chloroform) and poor (PS/MCH) solvent systems studied. Of these, PS/MCH showed the largest improvement, and PS/chloroform, the smallest (i.e. chloroform < toluene < MCH). Solvent quality of θ solvent systems

(PS/CH and PS/decalin at room temperature by SLS) deteriorated as applied pressure increased, with greater deterioration in PS/CH than in PS/decalin.

Decalin used in SLS measurements was a 50-50 mixture of *cis* and *trans* isomers. Others[10, 13-14] have used varying *cis,trans* isomer compositions in SLS dA_2/dP studies of PS/decalin at high pressure. Comparing our results with theirs will permit us to evaluate the effects of both isomer composition and pressure on decalin solvent quality.

Solvent quality trends in PS/decalin and other PS/organic solvent systems under pressure used in this project are discussed below in greater detail. By comparing our results to literature results, we find dA_2/dP often depends on the pressure range over which it is measured. In such systems, there is usually a steep change in dA_2/dP as the maximum applied pressure (P_{max}) increases, followed by a "leveling" or "plateauing" beyond some limiting $P_{max.}$[14]

For some of the PS/systems studied, we found no published dA_2/dP data with which to compare our results. In these cases, we compared general trends in solvent quality with applied pressure (dA_2/dP) to literature phase equilibria data (dT_{UCST}/dP). (When $dT_{UCST}/dP < 0$, $dA_2/dP > 0$ and solvent quality improves with applied pressure.)

Toluene. Of all solutions used in this work, only PS/toluene was studied using both membrane osmometry and static light scattering. The membrane osmometer was designed to operate in the low applied pressure region (0.1 - 6.0 MPa). We have compared second virial pressure coefficients obtained from MO to those obtained from SLS from ($0.1 \leq P_{applied}/MPa \leq 6.0$) and find that they are comparable (Table 3-1, p. 48).

Both are about 10^{-5} cm^3 mol g^{-2} MPa^{-1}, but the SLS pressure coefficient is much more precisely determined than the osmotic pressure coefficient.

Until now there has been relatively little work done in the low applied pressure region. Most light scattering studies of A_2 have been conducted over broad applied pressure ranges, with the spacing between data points at least 20 - 30 MPa. (e.g. A_2 measured at $P_{applied}$ = 0.1 MPa, 20 MPa, 40 MPa, etc.). Therefore, it is difficult to determine accurately the behavior of A_2 in the low applied pressure region (say 0.1 - 10 MPa applied) from these studies.

Figure 4-1 compares SLS dA_2/dP's from this work to those reported in the literature. The dA_2/dP data are plotted against the maximum applied pressure (P_{max}) at which they were acquired. Notice the downward curvature in the relationship of dA_2/dP to P_{max} from $\{6.0 \leq P_{max}/MPa \leq 80\}$. Above 80 MPa, there is essentially no change in dA_2/dP with further increase in P_{max}, even as the molecular weight of polystyrene increases ($100{,}000 \leq M_w \leq 1{,}800{,}000$ g/mol.)[10,14] Therefore, we conclude that $dA_2/dP_{PS/toluene}$ depends on the applied pressure region over which it is measured, and there is a threshold pressure (80 MPa) above which dA_2/dP is invariant.

Chloroform. Figure 4-2. shows the behavior of $dA_2/dP_{PS/chloroform}$ from ($35.0 \leq P_{max}/MPa \leq 400$). As in PS/toluene, the value of the second virial pressure coefficient of PS/chloroform depends on the applied pressure interval over which it is measured. dA_2/dP is small and positive at moderate applied pressure (35.0 MPa, this work) but nearly zero and essentially invariant from ($80 \leq P_{max}/MPa \leq 400$).[10, 14]

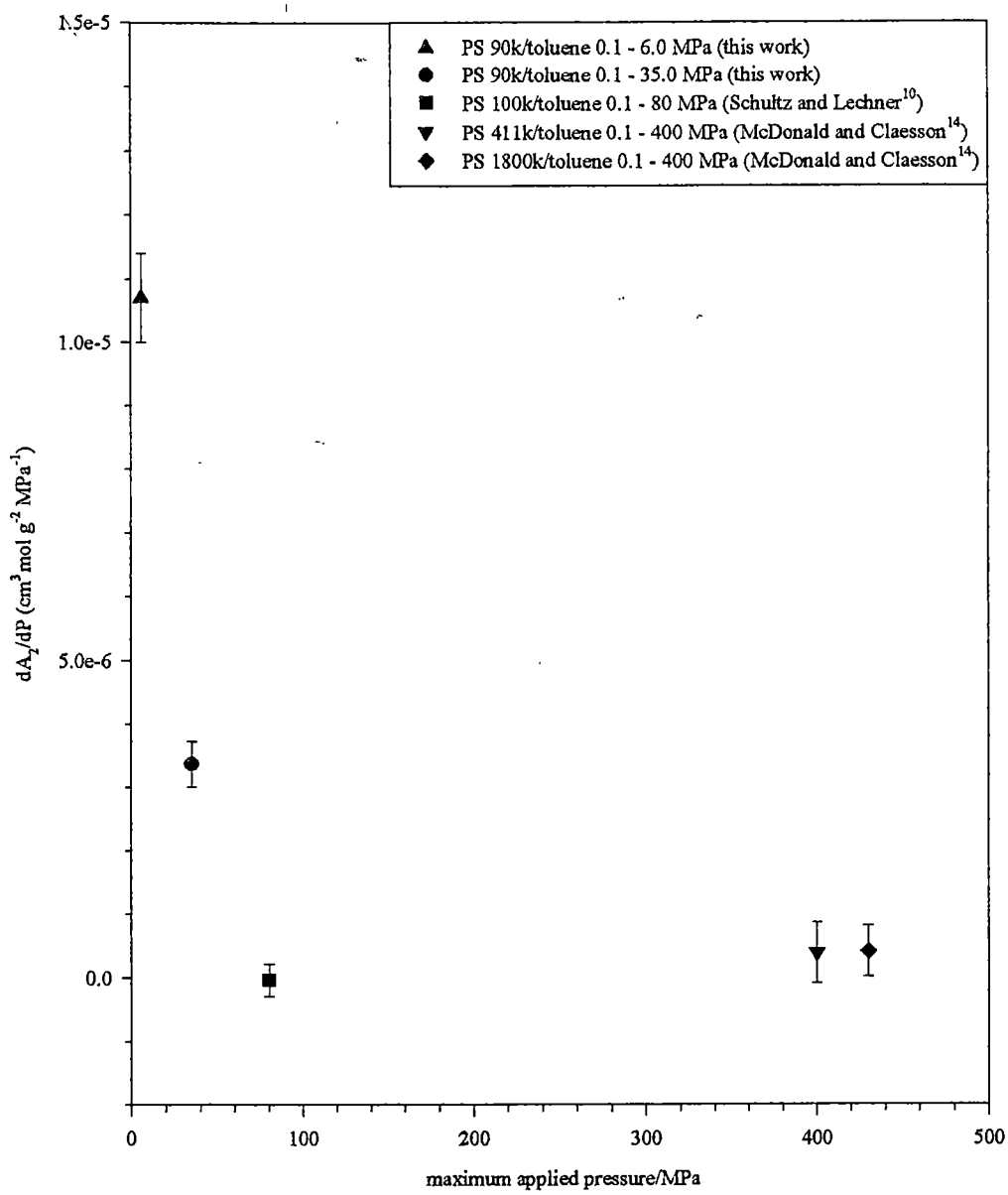

Figure 4-1. SLS dA_2/dP of PS/toluene.

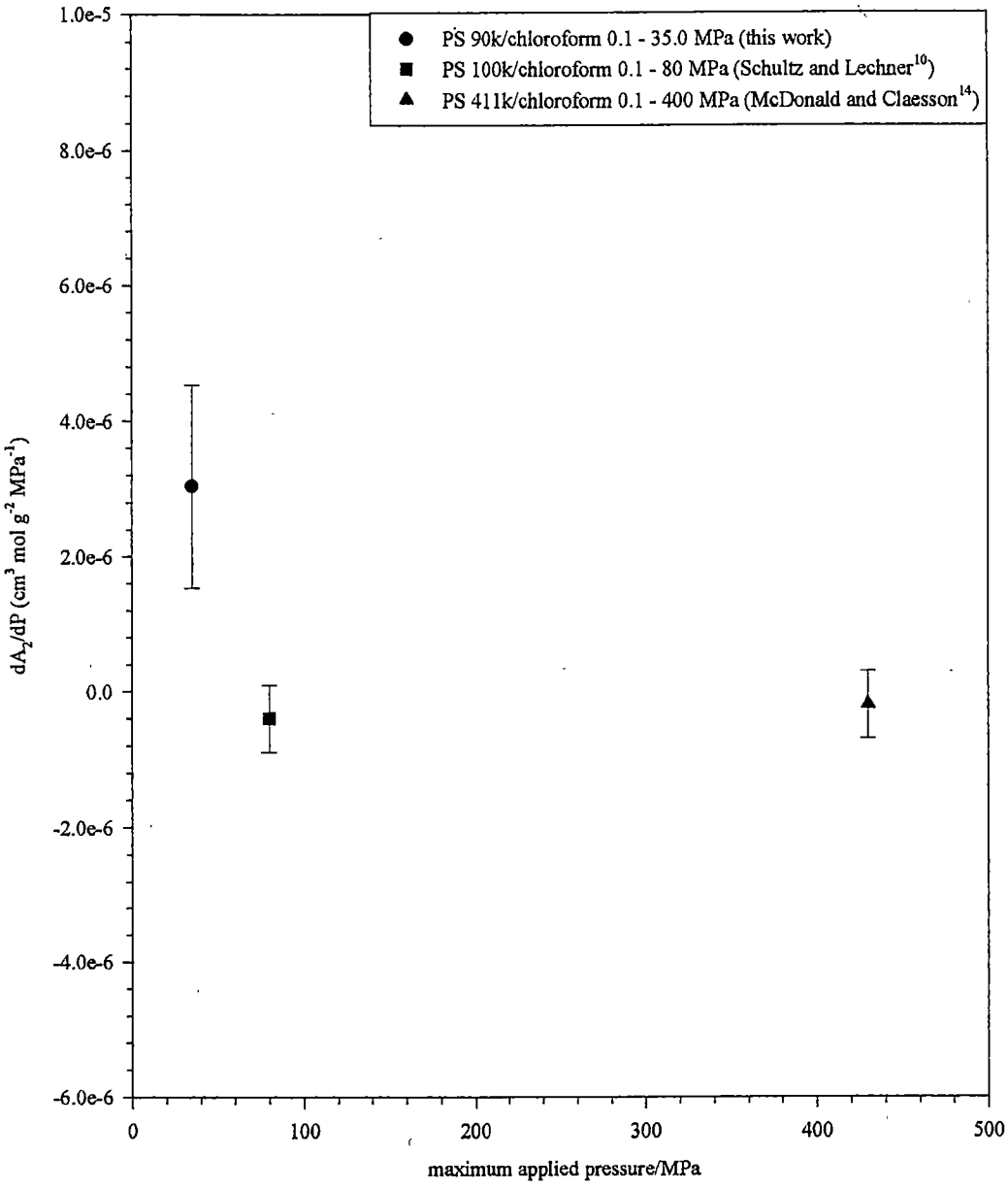

Figure 4-2. SLS dA_2/dP of PS/chloroform.

Interestingly, $dA_2/dP_{PS/chloroform} \cong dA_2/dP_{PS/toluene}$ ($0.1 \leq P_{applied}/MPa \leq 35.0$, this work) but the uncertainty in the chloroform pressure coefficient is ~ 65% larger than the uncertainty in the toluene coefficient. This uncertainty may be a result of the condition of the solvent, which we found difficult to clarify.

cis,trans-Decalin. The pressure coefficient (dA_2/dP) is sensitive to the isomeric composition of decalin. McDonald and Claesson[14] observed that $dA_2/dP_{PS\ 411k/decalin}$ is constant when *trans*-decalin content is less than or equal to 49% of the total volume of the solvent. Above 50% *trans,* the pressure coefficient becomes increasingly smaller and less negative, and in 100 % *trans*-decalin, $dA_2/dP^{14}_{PS\ 411k/decalin} \cong dA_2/dP^{10}_{PS\ 100k/decalin}$. (Schultz and Lechner[10] fit A_2 VS. P data to a second-order polynomial but did not list a numerical value of dA_2/dP in their paper. We replotted their data and fit them to a linear equation (for coherence sake) to obtain $dA_2/dP_{PS\ 100k/decalin}$.) Therefore, there is a small amount of upward curvature in the relationship of dA_2/dP to solvent composition[14] (Figure 4-3, filled triangles).

We have measured dA_2/dP of PS 90k in 50 % *trans*-decalin and plot our results along with literature results in Figure 4-3. For PS in 50% *trans*-decalin, the dA_2/dP we report (filled square) is smaller than either of McDonald and Claesson's measurements (filled triangles and diamonds), but this is due to the lower molecular weight polystyrene and lower applied pressure range used in our SLS measurements. McDonald and Claesson's data (dA_2/dP) for PS 411k and for PS 860k in 50% *trans*-decalin were measured over the same applied pressure range and are equivalent within experimental error.

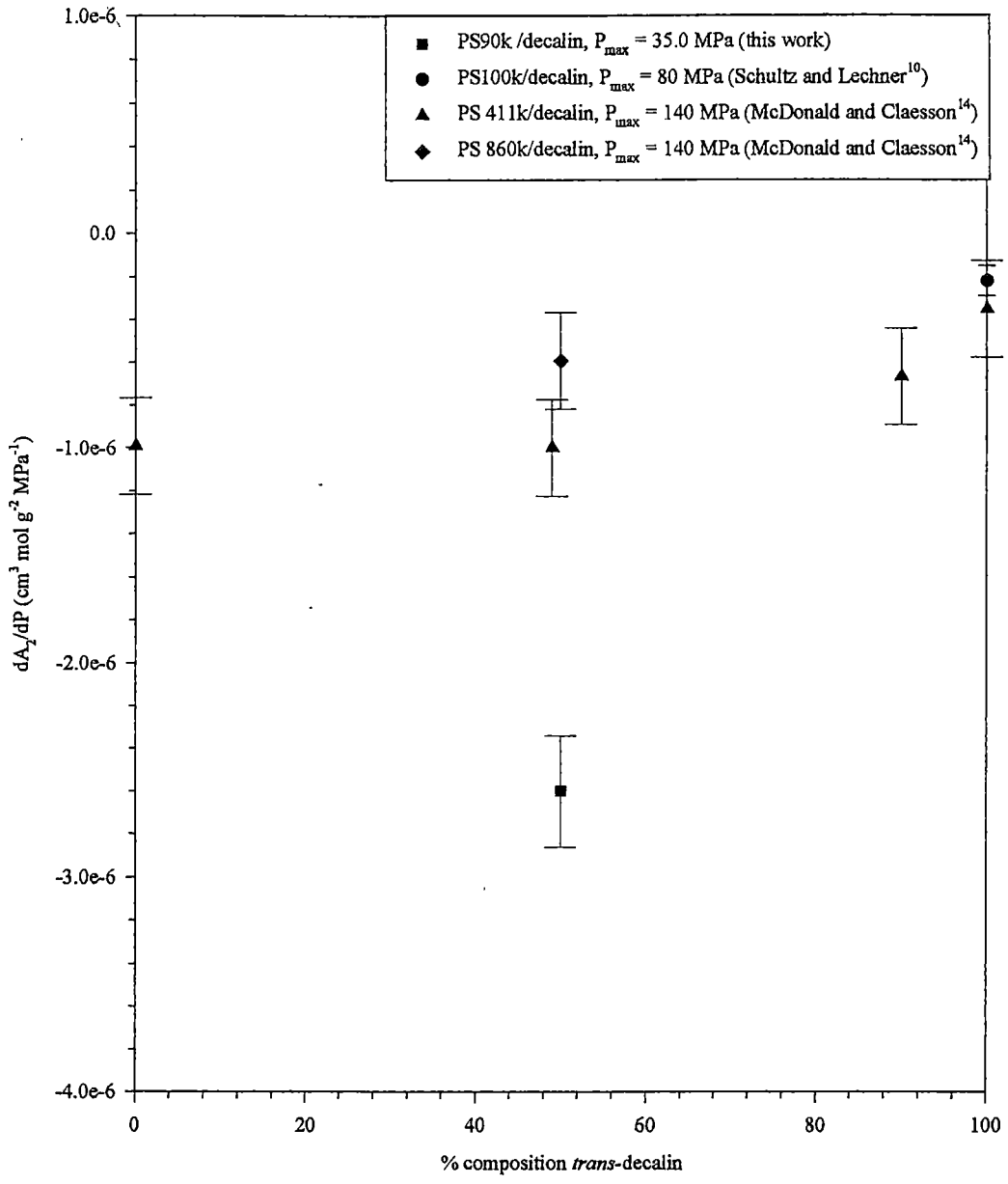

Figure 4-3. dA_2/dP of PS/decalin as a function of solvent composition.

MCH. Methylcyclohexane is a poor solvent for polystyrene and our results show that as applied pressure increases, MCH solvent quality in the system PS 25k/MCH improves ($dA_2/dP > 0$). The sign of dA_2/dP is related to the change in the upper critical solution temperature with applied pressure (i.e. dT_{UCST}/dP from demixing). When dA_2/dP is positive, and solvent quality improves with pressure, dT_{UCST}/dP is negative.

Demixing properties of PS/MCH systems under moderate pressure (to 40 MPa) have been reported in the literature. Imre and Van Hook[23] have observed a small improvement in solvent quality at low applied pressure (to 5.0 MPa) over a broad molecular weight range ($4{,}000 \leq M_w \leq 20{,}000{,}000$ g/mol). Others[47-49] have reported that solvent quality improves under moderate pressure (~ 40-50 MPa) when the molecular weight of PS is not too high ($9{,}000 \leq M_w \leq 34{,}900$ g/mol). These findings[23, 47-49] are in qualitative agreement with ours, which indicate that moderate pressure applied to PS 25k/MCH improves solvent quality.

Cyclohexane. Cyclohexane, a θ solvent (θ_{UCST} = 34 - 35°C) for polystyrene at atmospheric pressure, dissolves infinitely-long PS chains within a limited temperature range, which is bounded by upper and lower critical solution temperatures branches (θ_{UCST} and θ_{LCST}, respectively).[24] It is known that some θ solvents act like good solvents when the temperature is significantly different from θ_{UCST} and θ_{LCST} $\{T \geq (\theta_{UCST} + \theta_{UCST})/2\}$ or when the pressure is high enough.[43, 55-56] However, in other θ systems (e.g. PS/CH,[12,57] and PS/1-phenyldecane[12]) solvent quality improves under one set of experimental conditions ($P_{applied(1)}$, $T_{solution(1)}$) but deteriorates under another ($P_{applied(2)}$, $T_{solution(2)}$). In PS 25k/CH under moderate pressure (30.0 MPa), we observed solvent quality decreases

when $T_{solution} \leq 41°C$ but increases when $T_{solution} = 45°C$. Cyclohexane is a better solvent for PS 25k at ($T_{solution} = 45°C$, $0.1 \leq P_{applied}/MPa \leq 30.0$) than at ($T_{solution} = 41°C$, $0.1 \leq P_{applied}/MPa \leq 30.0$).

SLS measurements discussed above were made on a relatively low molecular weight polystyrene fraction (25,000 g/mol), but we also wanted to explore the pressure effect (i.e. dA_2/dP) in higher molecular weight systems. Light scattering measurements (~30°C, $0.1 \leq P_{applied}/MPa \leq 30.0$) were made on PS 400,000 g/mol and 900,000 g/mol in CH. $dA_2/dP_{PS\ 400k/CH}$ is positive and $dA_2/dP_{PS\ 900k/CH}$ is negative; therefore, solvent quality improves under one set of conditions ($M_w = 400{,}000$ g/mol; $T_{solution} \cong 30°C$; $0.1 \leq P_{applied}/MPa \leq 30.0$) but deteriorates as the molecular weight of PS increases. Saeki[57] also studied the effect of pressure on CH solvent quality in high molecular PS/CH solutions (via phase equilibria), but at lower applied pressure (0.1 - 5 MPa) than we used. Under these conditions, he found solvent quality increases as molecular weight increases ($110{,}000 \leq M_w \leq 1{,}450{,}000$ g/mol).

These results (ours as well as those in the literature) reiterate that solvent quality is a complex function of many variables whose effects are, in some cases, both interrelated and cumulative. We have examined but a few of these effects in PS/CH, as have others, choosing to devote most of our effort to understanding how pressure changes solvent quality. In the next section, we introduce a new variable —polymer architecture— and describe how SLS was used to study the interaction between linear and star polystyrenes at good, θ, and poor solvent conditions.

B. Second Virial Coefficients and Second Virial Cross Coefficients of Linear and Star Polystyrene Systems

Star polymers have arm-like branches that radiate from a central structure, and in the simplest case, each branch has approximately the same molecular weight. Studies indicate that θ_{UCST} decreases as the extent of branching increases (holding the total molecular weight of the polymer constant), and polymers with a large number of relatively short arms have the lowest θ temperatures of all. The depression of θ_{UCST} with branching is believed to result from the high segment density close to the central structure,[17, 58-59] and when the molecular weight of the polymer becomes large enough, θ_{UCST} reaches a finite limit.[46, 58]

No rigorous model has been developed to quantify the effect polymer architecture on A_2, but current evidence points to a decrease in the second virial coefficient as the extent of branching increases.[17] This effect is apparently due to changes in the mean square radius of gyration, $\langle R_g^2 \rangle$. Recent Monte Carlo and experimental studies of the behavior of nonlinear polymers in good solvents show that as the number of polymeric arms attached to the core increases, $\langle R_g^2 \rangle$ decreases, and from the value of the penetration function ψ ($\psi \sim A_2/\langle R_g^2 \rangle$), it follows that A_2 also decreases.[30, 60-63] Current A_2 results presented in Chapter 3 for linear and star polystyrene ($M \cong 400{,}000$ g/mol, near 25°C) in toluene are in qualitative agreement with literature values.

Second virial coefficients reported in this work for linear ($A_{2(L\text{-}L)}$) and star ($A_{2(S\text{-}S)}$) PS dissolved (separately) in cyclohexane (θ solvent) and methylcyclohexane (poor solvent) are the same within experimental error. Since some high molecular weight,

highly-branched polymers are known not to dissolve in θ solvents,[17] we investigated solubility differences between 8-arm star polystyrene and linear polystyrene (of comparable molecular weight) in CH and MCH. Cloud point measurements (Figures 3-11 and 3-12, pp. 55-56) indicate that star PS 417k is slightly more soluble than linear PS 400k in both solvents, but the difference ($UCST_{\text{linear PS}} - UCST_{\text{star PS}} = \Delta UCST$) is small (~3°). Therefore, there is no indication from these solubility data that $A_{2(L\text{-}L)}$ should differ significantly from $A_{2(S\text{-}S)}$ in CH or MCH.

Second virial cross coefficients between (architecturally) different polymers dissolved in the same solvent are measures of the extent of polymer-polymer interaction. In Figure 3-10 (p. 52), second virial coefficients of linear-star PS mixtures in toluene, CH, and MCH are plotted, and data are fit to a three parameter equation (eq. 3-7, p. 50) of the form

$$f = (1\text{-}S)^2B + S^2C + 2S(1\text{-}S)D$$

in which S = weight fraction of 8-arm star PS 417k, $B = A_{2(L\text{-}L)}$, $C = A_{2(S\text{-}S)}$, and $D = A_{2(L\text{-}S)}$. This equation fits PS/toluene data (Figure 3-10 (A), p.52) fairly well, giving a negative value of $A_{2(L\text{-}S)}$ on the order of -3.0×10^{-4} cm^3 mol g^{-2} MPa^{-1}. Therefore, linear-star PS interactions are preferred over linear PS-toluene and star PS-toluene interactions.

In PS/CH mixtures (Figure 3-10(B), p.52), however, our data show second virial coefficients are independent of relative amounts of linear and star PS in solution, and within experimental error $A_{2(L\text{-}L)} = A_{2(S\text{-}S)} = A_{2(L\text{-}S)}$. Therefore, linear-star PS interactions are negligible in this system.

$A_{2(L-L)}$ and $A_{2(S-S)}$ are equivalent within experimental error in linear-star PS/MCH mixtures (Figure 3-10(C), p. 52). Over the (0.25 - 0.65) star-PS weight fraction interval, there is quite a bit of scatter in A_2 values. Equation (3-7) does not accurately describe linear-star PS interactions in MCH, and we conclude that it is not possible to assign an accurate value of $A_{2(L-S)}$ to linear-star PS/MCH from these data.

Striolo and Prauznitz [30] found from membrane osmometry studies that in lower molecular weight PS systems (i.e. ~74,000 g/mol linear PS and 8-arm star PS fractions), second virial cross coefficients ($A_{2(L-S)}$) in toluene, CH, and MCH are positive, and each $A_{2(L-S)}$ lies between the second virial coefficients ($A_{2(L-L)}$ and $A_{2(S-S)}$). Differences between these results and ours are likely due to the different molecular weights of polymers used in each study and to the different techniques (membrane osmometry VS. SLS) used to measure second virial coefficients. Uncertainties in CH and MCH cross virial coefficients (100 and 130%, respectively) are much larger than the uncertainty in the toluene system cross coefficient (15%).[30] The same trend in uncertainties was also present in the linear + star PS systems we studied.

Chapter 5

Conclusion

We have measured the change in the second virial coefficient of dilute polystyrene solutions with respect to applied pressure (dA_2/dP) using membrane osmometry (0.1 - 6.0 MPa) and static light scattering (0.1 - 35.0 MPa). Results have been interpreted in terms of the change in solvent quality with applied pressure, and static light scattering data have been compared to literature values. To our knowledge, we have made the first such measurements on dilute polystyrene solutions under pressure using membrane osmometry and find that SLS is advantageous to membrane osmometry as a rapid, convenient method of obtaining second virial pressure coefficients to useful precision.

Solvent quality in good and poor solvent systems near 25°C (PS/toluene and PS/chloroform; PS/MCH, respectively) improves under moderate applied pressure ($0.1 \leq P_{applied}/MPa \leq 35.0$). Improvement is greatest in MCH, least in chloroform (MCH > toluene > chloroform). In θ solvent systems near 25°C (PS/CH, PS/50-50 *cis,trans*-decalin), solvent quality deteriorates under pressure (CH deterioration > decalin deterioration). In PS/decalin, solvent quality deterioration is a function not only of applied pressure, temperature and molecular weight but also of the isomeric composition of the solvent.[14] (McDonald and Claesson's work[14] shows that as the cis/trans ratio decreases, decalin solvent quality as a function of pressure increases.)

Changes in solvent quality (improvement or deterioration) are not necessarily constant across a broad range of applied pressure. Solvent quality may improve at low pressure then decline at high pressure (or vice versa) or improve at low pressure then

reach a plateau. For example, toluene solvent quality (PS/toluene) increases under low-to-moderate applied pressure ($P_{applied}$/ MPa = 0.1 - 6.0 and 0.1 - 35.0 MPa; this work) then plateaus above 80 MPa.[10, 14]

We measured the effects of temperature and molecular weight on solvent quality in PS/CH systems to demonstrate the simultaneous dependence of solvent quality on many different variables. Our results show cyclohexane solvent quality declines with applied pressure ($0.1 \leq P_{applied}/MPa \leq 30.0$) in low molecular weight PS (25,000 g/mol) solutions until far above room temperature, at which point (45°C) solvent quality increases with pressure. When molecular weight is high (400,000 g/mol) and temperature is slightly above room temperature (30°C), cyclohexane solvent quality also improves under moderate pressure. However, doubling the molecular weight of the polymer (holding temperature constant, and over the same applied pressure range) brings about a decline in solvent quality.

In a related study, we measured the effect of polymer architecture on polymer-polymer interactions in dilute solution. Second virial cross coefficients of linear-star PS mixtures in toluene (good solvent), CH (θ solvent), and MCH (poor solvent) at atmospheric pressure were measured using SLS. Our results show that there is a small amount of linear-star PS interaction in the good solvent but none in the θ or poor solvent. In lower molecular weight systems, there is some evidence[30] that linear PS-solvent and star PS-solvent interactions are preferred.

The majority of this work was devoted to understanding how pressure affects solvent quality in polystyrene solutions. In one system (PS/CH), we have also examined

other variables (temperature, molecular weight) in conjunction with pressure. We know that solvent quality is not defined by a *single* variable but is influenced in a complex way by many different variables such as pressure, temperature, molecular weight, concentration, polymer architecture, etc. It is our hope that the results discussed in this study not only extend what is known about the thermodynamic behavior of polymer solutions under pressure but also provide some understanding of the cumulative impact of different variables on solvent quality.

References

References

1. van't Hoff, J.H., *Z. Phys. Chem.*, **1,** (1887).
2. Postnjak, E., *Kolloidchem. Beih.*, **3,** 417 (1912).
3. Ostwald, W. and Mundler, K., *Kolloid Z.*, **24,** (1919).
4. Schultz, G.V., *Z. Phys. Chem. A.*, **158,** 237 (1932).
5. Adair, G.S., *Proc. R. Soc. A.*, **120,** 573 (1928).
6. Haller, W., *Kolloid Z.*, **56,** 257 (1931).
7. Duclaux, J. and Wollman, E., *Compt. Rend.*, **152,** 1580 (1911).
8. Caspari, W.A., *J. Chem. Soc.*, **105,** 2139 (1914).
9. Brandrup, J. and Immergut, E.H., Eds., *Polymer Handbook,* 3rd ed., John Wiley & Sons, New York (1989).
10. Lechner, M. and Schultz, G.V., *Eur. Polym. J.*, **6,** 945 (1970).
11. Gaeckle, D., and Patterson, D., *Macromolecules,* **5,** 136 (1972).
12. Wolf, B.A. and Geerissen, H., *Colloid & Polym. Sci.*, **259,** 1214 (1981).
13. McDonald, C.J. and Claesson, S., *Chemica Scripta,* **4,** 155 (1973).
14. McDonald, C.J. and Claesson, S., *Chemica Scripta,* **9,** 36 (1976).
15. Kubota, K., Kubo, K., and Ogino, K., *Bulletin of the Chemical Society of Japan,* **49,** 2410 (1976).
16. Charmasson, R. and Catella, R., *Eur. Polym. J.*, **8,** 697 (1972).
17. Kratochivil, P., *Classical Light Scattering from Polymer Solutions,* Elsevier, New York (1987).
18. Flory, P.J., *Principles of Polymer Chemistry,* Cornell University Press, Ithaca, NY (1953).
19. Painter, P.C. and Coleman, M.M., *Fundamentals of Polymer Science,* Technomic, Lancaster, PA (1997).
20. deGennes, P.G., *Scaling Concepts in Polymer Physics,* Cornell University Press, Ithaca, NY (1979).
21. Flory, P.J. and Krigbaum, W.R., *J. Chem. Phys.*, **18,** 1086 (1950).

22. Imre, A. and Van Hook, W.A., *J. Polym. Sci. B. Polym. Phys.*, 35, 1251 (1997).

23. Imre, A. and Van Hook, W.A., *J. Phys. Chem. Ref. Data,* **25,** 637 (1996).

24. Imre, A. and Van Hook, W.A., *Recent Res. Devel. Polym. Sci.*, **2,** 539 (1998).

25. Klotz, I.M. and Rosenberg, R.M., *Chemical Thermodynamics. Basic Theory and Methods,* 5th ed., John Wiley & Sons, NewYork (1994).

26. Tanford, C., *Physical Chemistry of Macromolecules,* John Wiley & Sons, New York (1961).

27. Des Cloizeaus, J. and Jannink, G., *Polymers in Solution,* Clarendon Press, Oxford, UK (1991).

28. Sydlowski, J. and Van Hook, W.A., *Macromolecules,* **31,** 3266 (1998).

29. Stockmayer, W.H., *J. Chem. Phys.*, **18,** 58 (1950).

30. Striolo, A. and Prausnitz, J.M., *J. Chem. Phys.*, **113,** 2927 (2000).

31. Kamide, K., *Thermodynamics of Polymer Solutions. Phase Equilibria and Critical Phenomena,* Elsevier, New York (1990).

32. Dry membranes were soaked in a series of water/isopropanol solutions (75/25% - 100/0% respectively) for at least two hours each, then conditioned to the solvent to be used (75/25% - 0/100% isopropanol/solvent, respectively).

33. Heller, W., *J. Polym. Sci.: part A-2,* **4,** 209 (1966).

34. The cell was originally designed to function at a maximum applied pressure of 200 MPa, thus requiring sapphire windows (rather than Pyrex) to withstand such pressures. While it would be ideal to use sapphire capillary in light scattering measurements to cover range of scattering angles, the price of optical-quality sapphire is prohibitive and would require the use of very small-diameter capillaries. Unfortunately, the refractive index of sapphire is too high to allow for refractive index matching at high (capillary) curvature (i.e. in small-diameter capillary) where stray reflections are most problematic. Van Hook, Wilczura, and Rebelo[33] have found that flat sapphire windows are easier to obtain and more economical to use in light scattering than sapphire capillaries.

35. Van Hook, W.A., Wilczura, H., and Rebelo, L.P.N., *Macromolecules,* **32,** 7299 (1999).

36. $t = \left[\frac{100(R_t - 100.344)}{38.286} + 1.95\left(\frac{t}{100} - 1\right)\left(\frac{t}{100}\right) \right]$ in which t = temperature/°C and R_t = resistance (Ω).

37. Flory, P.J.and Daoust, H., *J. Poly. Sci.,* **25,** 429 (1957).

38. Krigbaum, W.R. and Flory, P.J., *JACS,* **75,** 1775 (1953).

39. Bawn, C.E.H., *Trans. Faraday Soc.,* **46,** 980 (1950).

40. Schick, M.J., Doty, P., and Zimm, B.H., *JACS,* **72,** 530 (1950).

41. Bawn, C., Freeman, R., and Kamaliddin, A., *Trans. Faraday Soc.,* **46,** 862 (1950).

42. Sourirajan, S., *J. Appl. Chem.,* **14,** 506 (1964).

43. Krigbaum, W.R. and Carpenter, D.K., *J. Phys. Chem.,* **59,** 1166 (1955).

44. Krigbaum, W.R. and Flory, P.J., *J. Polym. Sci.,* **11,** 37 (1953).

45. Outer, P., Carr, C.I, and Zimm, B.H., *J. Chem. Phys.,* **18,** 830 (1950).

46. Striolo, A., Prausnitz, J.M., and Bertucco, A., *Macromolecules,* **33,** 9583 (2000).

47. Hosokawa, H., Nakata, N., and Dobashi, T., *J. Chem. Phys.,* **98,** 10078 (1993).

48. Wells, P.A., de Loos, Th. W., and Kleintjens, L.A., *Fluid Phase Equilibria,* **83,** 383 (1993).

49. Vanhee, S., Kiepen, F., Brinkmann, D., Borchard, W., Koningsveld, R., and , Berghmans, H., *Makromol. Chem., Phys.,* **195,** 759 (1994).

50. Imre, A. and Van Hook, W.A., *J. Polym. Sci.,* **B34,** 751 (1996).

51. Saeki, S., Kuwahara, N., and Kaneko, M., *Macromolecules,* **24,** 4883 (1991).

52. Zeman, L. and Patterson, D., *J. Phys. Chem.,* **76,** 1214 (1972).

53. Imre, A. and Van Hook, W.A., *J. Polym. Sci.,* **B32,** 2283 (1994).

54. Instruction Manual for BI-200SM Goniometer, Version 2.0

55. Krigbaum, W.R., *J. Am. Chem. Soc.,* **76,** 3758 (1954).

56. Lechner, M.D., Schultz, G.V., and Wolf, B.A., *J. Coll. Interface Sci.*, **39,** 462 (1972).

57. Saeki, S., Kuwahara, N., Nakata, M., and Kaneko, M., *Polymer,* **16,** 445 (1975).

58. Ganazzoli, F. and Allegra, G., *Macromolecules,* **0,** 262 (1990).

59. Okumoto, M., Terao, K., Nakamura, Y., Norisuye, T., and Teramoto, A., *Macromolecules,* **30,** 7493 (1997).

60. Ohno, K., Shida, K., Kimura, M., and Kawazoe, Y., *Macromolecules,* **29,** 2269 (1996).

61. Grest, G.S., Fetters, L.J., Huang, J.S., and Richter, D., *Adv. Chem. Phys.*, **94,** 67 (1996).

62. Douglas, J.F., Roovers, J., and Freed, K.F., *Macromolecules,* **23,** 4168 (1990).

63. Okumoto, M., Nakamura, Y., Norisuye, T., and Teramoto, A., *Macromolecules,* **31,** 1615 (1998).

Appendices

Appendix 1

Modified from the IEEE488 Device Driver Example Program RD705196

QuickBasic 4.0

Serial Poll with DMA transfer

MetraByte Corporation

```
'This program controls Keithley 705 scanner which in turn runs the Keithley 196 DVM
'using any of ten channels.  The 705 is DEVICE #17; the 196 is DEVICE #7.

DECLARE SUB ADDRESS (dma%( ), COUNT%, ADDR%)
DIM da(500,8) 'The data array is a 500 row by 8 column array
DIM DV%(100)

GOSUB 11000
PRINT "Enter filename"
INPUT NN$
PRINT "Describe this run"
INPUT DSCRP$
PRINT "Enter the pressure in MPa"
INPUT PRES$

j = 1
        DO
                For j = 1 to 499

A$ = INKEY$
REM A$ = "s or shift s" entered will transfer control to 15000 for data storage followed
REM by program termination.
IF A$ = "s" OR A$ = "S" THEN GOSUB 15000

CALL ADDRESS (DV% ( ), 100, ADDR%) 'Calculate address within DV% that lies on
'a page boundary
DEF SEG = ADDR% 'Set reference segment for peek and poke functions

'#### Establish communication with device driver ####

100 OPEN "$DV488" FOR OUTPUT AS #1
101 PRINT #1, "BUFFERCLEAR"
102 OPEN "$DV488" FOR INPUT AS #2
103 ON ERROR GOTO ersvc
```

```
'#### Initialize MBC-488 board using "SYSCON" command ####

200 PRINT #1, "SYSCON MAD1=3  CIC1=1  BA1=&H300"

'#### Set DVM into REMOTE ####
'Section which calls 705 channels successively

300 START = TIMER
310 PRINT #1, "REMOTE 17" 'puts the Model 705 scanner into remote mode
320 CMD$ = "N1C2N3N4N5N6N7N8N9N10B1X"
'N = open, #s refer to channels, C = close, B = display, X = execute
330 PRINT #1, "OUTPUT 17 $ +", CMD$
340 PRINT #1, "REMOTE 7" 'puts the model 196 DMM into remote

'#### SET MODE TO TRIGGER ON "GET" ####
400 TCONF = TIMER
410 CMD$ = "T3F2R1S3G1M8X"
'T3 = one shot on GET, F2 = ohms, R0 = autoscale, S3 = resolution, M8 = buffer half
'full, X = execute, G1 = channel data sent without prefix
420 PRINT #1, "OUTPUT 7 $ +" CMD$
'It takes 0.3 seconds for the 196 to process the command string.
430 GOSUB 44444
'#### Send trigger message ####
440 PRINT #1, "TRIGGER 7"
'#### Wait for SRQ ####

450 REQ% = 0
460 WHILE (REQ% AND &H4000) <> &H4000
470 PRINT #1, "REQUEST"
480 INPUT #2, REQ%
490 WEND

'#### Read serial poll byte ####
500 PRINT #1, "STATUS 7"
510 INPUT #2, SPOLL%
520 IF (SPOLL% AND 8) <> 8 THEN PRINT "No request in Serial Poll Byte":  STOP

'#### Read data from DVM ####
530 PRINT #1, "ENTER 7 DMA", ADDR%, "0", 16

'#### Wait for DMA to finish ####
540 REQ% = &H200
```

```
550 WHILE (REQ% AND &H200) = &H200
560 PRINT #1, "REQUEST"
570 INPUT #2, REQ%
580 WEND
590 DV$ = "" 'clear a string for printing returned data
600 FOR OFFS = 0 TO 10 'recover stored DMA data
610 DV$ = DV$ + CHR$ (PEEK(OFFS))
620 NEXT OFFS
630 OHMS = VAL(MID$(DV$, 2, 8)) 'returns the numerical value of the voltage DMM
'string starting at the second digit in the string and returning that digit plus the next 8
'digits to the right for a total of 9 characters
650 da (j, 1) = OHMS
660 T$ = TIME$
670 Hr = VAL (T$)
680 If Hr < 12 THEN Ampm$ = "AM" ELSE Ampm$ = "Pm"
690 If Hr > 12 then Hr = Hr - 12
700 PRINT "The time is"; STR$(Hr); RIGHT$(T$, 6); Ampm$
710 Min = VAL(MID$(T$, 4, 2)):  Sec = VAL(RIGHT$(T$, 2))
720 da(j, 2) = Hr
730 da(j, 3) = Min
740 da(j, 4) = Sec
750 PRINT "j = "; j ' "da(j, 1) = ", da(j, 1); Hr; ":"; Min; ":"; Sec
760 CH1$ = DV$
770 T1END = TIMER
790 CLOSE
800 PRINT " CH1$ = "; CH1$

'#### Delay loop so we can read output data ####
820 FOR A = 1 TO 5000
830 NEXT A
840 CALL ADDRESS (DV%( ), 100, ADDR%) 'Calculate address within DV% ( ) that
'lies on a page boundary
850 DEF SEG = ADDR% 'Set reference segment for peek and poke functions

'#### Establish communication with device driver ####
860 OPEN "$DV488" FOR OUTPUT AS #1
870 PRINT #1, "BUFFERCLEAR"
880 OPEN "$DV488" FOR INPUT AS #2
890 ON ERROR GOTO ersvc

'#### Initialize MBC-488 board using "SYSCON" command ####
900 PRINT #1, "SYSCON MAD1=3  CIC1=1  BA1=&H300"
```

```
'#### Set DVM into REMOTE ####
'Section which calls 705 channels successively
910 START = TIMER
920 PRINT #1, "REMOTE 17"
930 CMD$ = "C1N2N3N4N5N6N7N8N9N10B2X"
'N = open, #s refer to channels, C = close, B = display, X = execute
940 PRINT #1, "OUTPUT 17 $ +", CMD$
950 PRINT #1, "REMOTE 7"

'#### Set mode to trigger on "GET" ####
960 TCONF = TIMER
970 CMD$ = "T3F0R2S3G1M8X"
'T3 = one shot on GET, F0 = DC volts, R2 = 2V scale, S3 = 20 - 16.6 millisecond
'resolution, G1 = channel data sent without prefix, M8 = buffer half full, X = execute
980 PRINT #1, "OUTPUT 7 $ +", CMD$
990 GOSUB 44444

'#### Send trigger message ####
1000 PRINT #1, "TRIGGER 7"

'#### Wait for SRQ ####
1010 REQ% = 0
1020 WHILE (REQ% AND &H4000) <> &H4000
1030 PRINT #1, "REQUEST"
1040 INPUT #2, REQ%
1050 WEND

'#### Read serial poll byte ####
1060 PRINT #1, "STATUS 7"
1070 INPUT #2, SPOLL%
1080 IF (SPOLL% AND 8) <> 8 THEN PRINT "No request in serial poll byte": STOP

'#### Read data from DVM ####
1090 PRINT #1, "ENTER 7 DMA", ADDR%, "0", 17

'#### Wait for DMA to finish ####
1100 REQ% = &H200
1110 WHILE (REQ% AND &H200) = &H200
1120 PRINT #1, "REQUEST"
1130 INPUT #2, REQ%
1140 WEND
1150 DV$ = "" 'clear a string for printing returned data
1160 FOR OFFS = 0 TO 20 'recover stored DMA data
```

```
1170 DV$ = DV$ + CHR$ (PEEK(OFFS))
1180 NEXT OFFS
1190 VOLTAGE = VAL(MID$(DV$, 1, 11))
1201 da (j, 5) = VOLTAGE
T$ = TIME$
Hr = VAL(T$)
IF Hr < 12 THEN Ampm$ = "AM" ELSE Ampm$ = "Pm"
IF Hr > 12 THEN Hr = Hr - 12
PRINT "The time is"; STR$(Hr); RIGHT$(T$, 6); Ampm$; Min = VAL(MID$(T$, 4,
      2)):  Sec = VAL(RIGHT$(T$, 2))
da (j, 6) = Hr
da (j, 7) = Min
da (j, 8) = Sec
1210 PRINT "j= "; j ' "da (j, 5) ="; da (j, 5); Hr; ":"; Min; ":"; Sec
1220 CH2$ = DV$
1230 CLOSE
1240 PRINT " CH2$ = "; CH2$

'#### Delay loop so we can read output data ####
1241 FOR A = 1 TO 500000
1242 NEXT A
1250 FOR b = 1 TO 500000
1260 NEXT b

        NEXT j
     EXIT DO
LOOP UNTIL j = 499
GOSUB 15000

CLOSE
STOP

ersvc:
IF (ERR <> 68) AND (ERR <> 57) THEN PRINT "BASIC ERROR # "; ERR; " IN
      LINE "; ERLS:  STOP
INPUT #2, e$
PRINT "$DV488 driver returned error number - ", e$
INPUT #2, e$
PRINT e$
INUT #2, e$
PRINT e$
END
```

```
11000 PRINT ""
11837 PRINT "%%%%%%%%%%%%%%%%%%%%"
11838 PRINT ""
11840 PRINT "This program is stored in **\QB45\OSMO**"
11850 PRINT "We now change to **\QB45\OSMO\DATA** to store data"
11860 CHDIR "C:\QB45\OSMO\DATA"

15000 'This routine stores data files
15070 EXT$ = ".RAW"
15080 N$ = NN$ + EXT$
15110 OPEN N$ FOR OUTPUT AS #3
15125 PRINT #3, "File name is      "; N$
15126 PRINT #3
15130 PRINT #3, "DSCRP$ is      "; DSCRP$
15135 DTEEXP$ = DATE$
15136 PRINT #3, "The date of this run is          "; DTEEXP$
15137 PRINT #3, "The ending time for this run is      "; STR$ (Hr); RIGHT$ (T$, 6);
      Ampm$; Min = VAL(MID$(T$, 4, 2)):  Sec = VAL(RIGHT$(T$, 2))
15150 PRINT #3, JK$, 'JK
15155 AB = j
15160 PRINT #3, "Number of data points is    "; AB
15170 PRINT #3, "The pressure in MPa at which this run is conducted is    "; PRES$
15175 PRINT #3, ""
15180 PRINT #3, "Ohms          Min Sec          Volts          Min Sec          "
15190 PRINT #3, ""
15200 FOR I = 1 TO AB
15300 PRINT #3, USING "###.####          ## ##     ##.######     ## ## "; da (I, 1);
      da (I, 3); da (I, 4); da (I, 5); da (I, 7); da (I, 8)
15310 NEXT I
15320 CLOSE #3
15480 j = 1
15490 IF AB = 6 THEN GOTO 15900
15900 CLS
15910 PRINT "##################################"
15920 PRINT "I have collected and stored all data points"
15959 END

44444 TCONF2 = TIMER
      IF TCONF2 - TCONF > 0.3 THEN 44448
44448 RETURN

SUB ADDRESS (dma% ( ), COUNT%, ADDR%)
'subroutine to allocate space for DMA transfers
```

```
DIM A AS LONG
DIM b AS LONG

        CLS

        S = VARSEG (dma% (0))   'get segment address
        o = VARPTR (dma% (0))  'get segment offset

        IF o < 0 THEN o = o + 65536
        IF S < 0 THEN S = S + 65536

        A = S * 16 + o

        page = INT (A / 65536)

        REM  See if there will be a DMA WRAP AROUND

        b = A - (page * 65536)
        b = b + COUNT%

        IF b > 65535 THEN
                ADDR% = (page + 1) * 4000:  REM here if page wrap would occur
        ELSE REM here if no page wrap
                A = A / 16
                IF A > 32767 THEN ADDR% = A - 65536
                ELSE ADDR% = A
        END IF

END SUB
```

Appendix 2

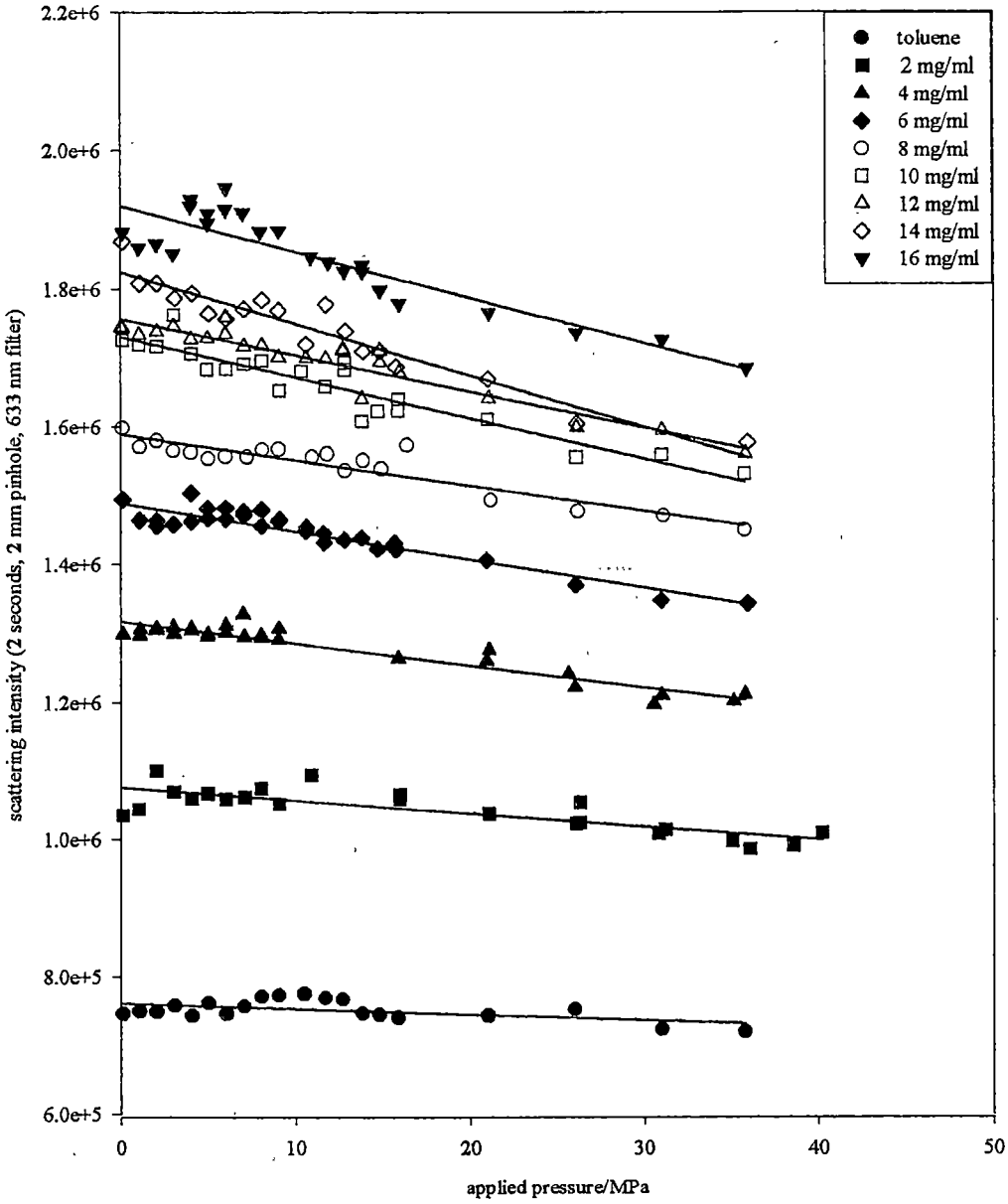

Scattering intensity of PS 90k in toluene as a function of applied pressure

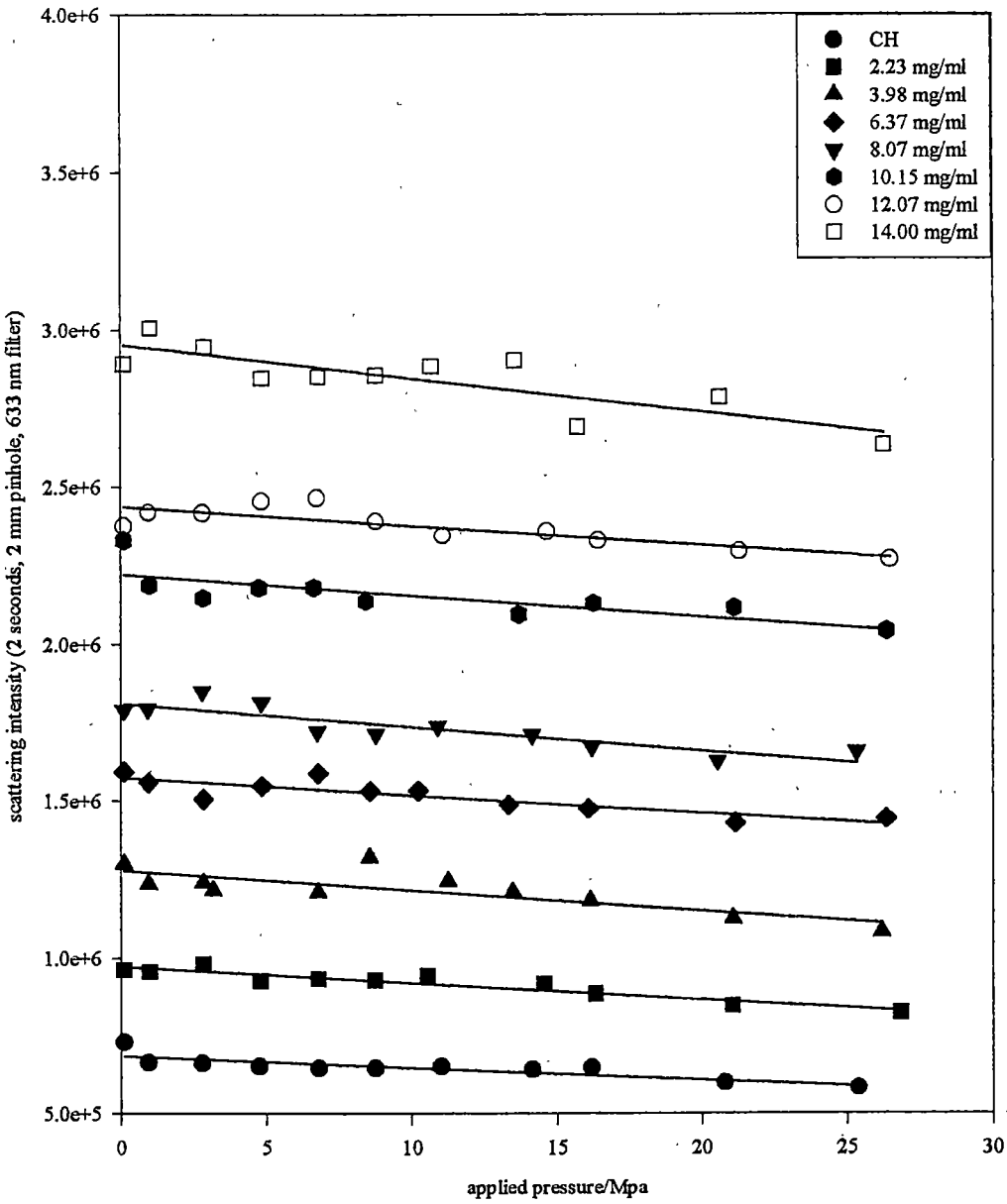

Scattering intensity of PS 25k in CH at 22 °C as a function of applied pressure

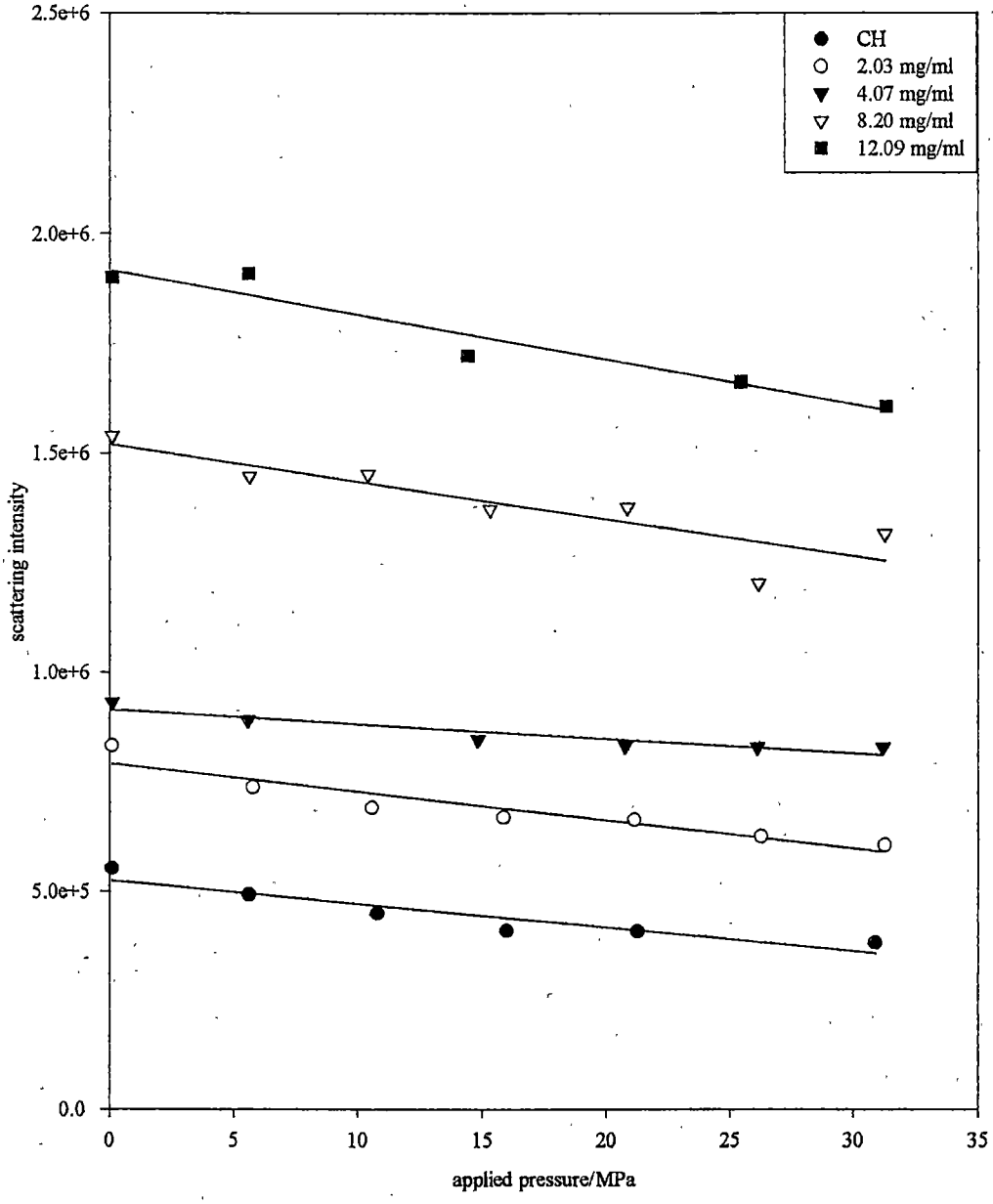

Scattering intensity of PS 25k in CH at 41 °C as a function of applied pressure

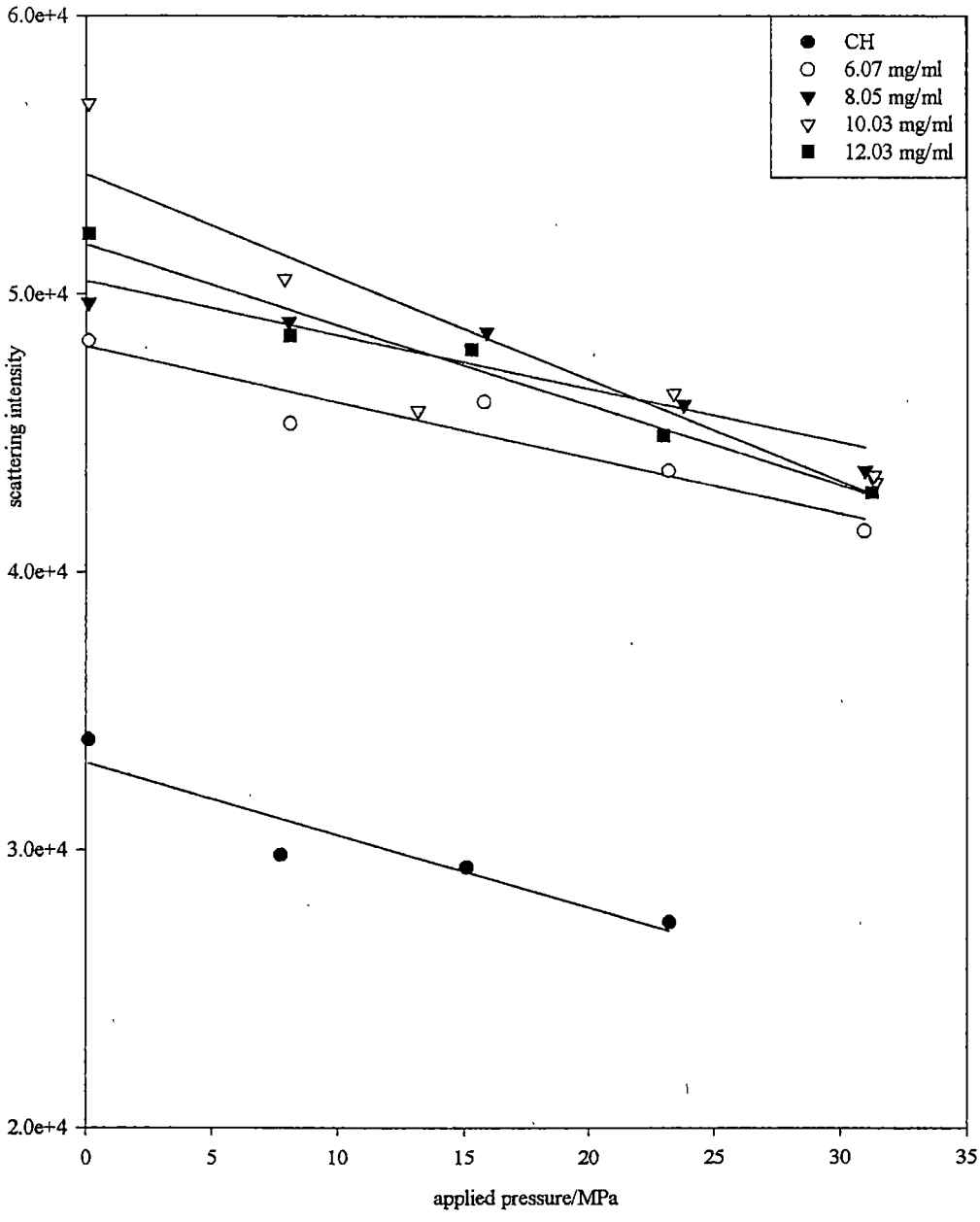

Scattering intensity of PS 25k in CH at 45 °C as a function of applied pressure

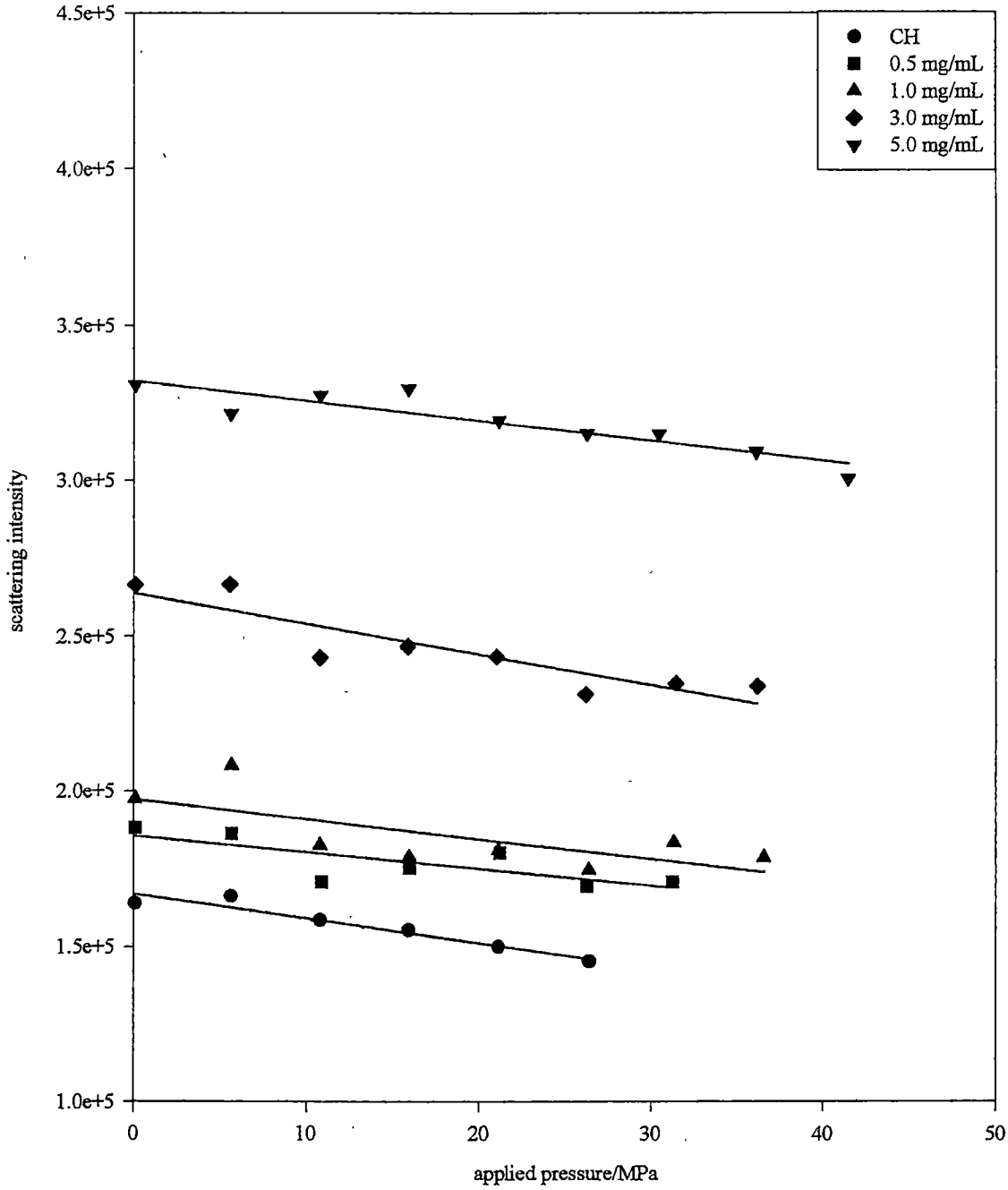

Scattering intensity of PS 400k in CH at 27.4°C as a function of applied pressure.

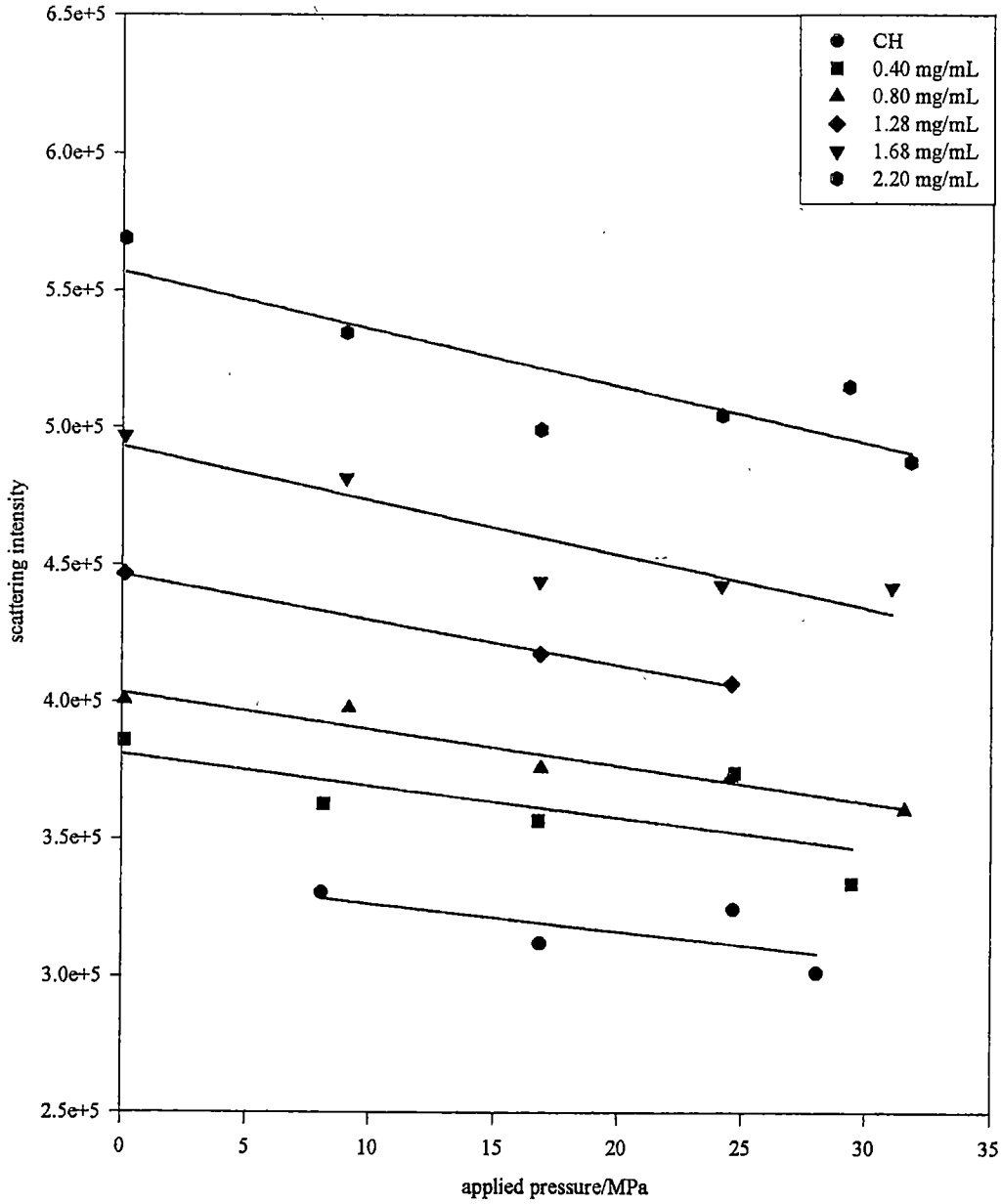

Scattering intensity of PS 900k in CH at 29°C as a function of applied pressure

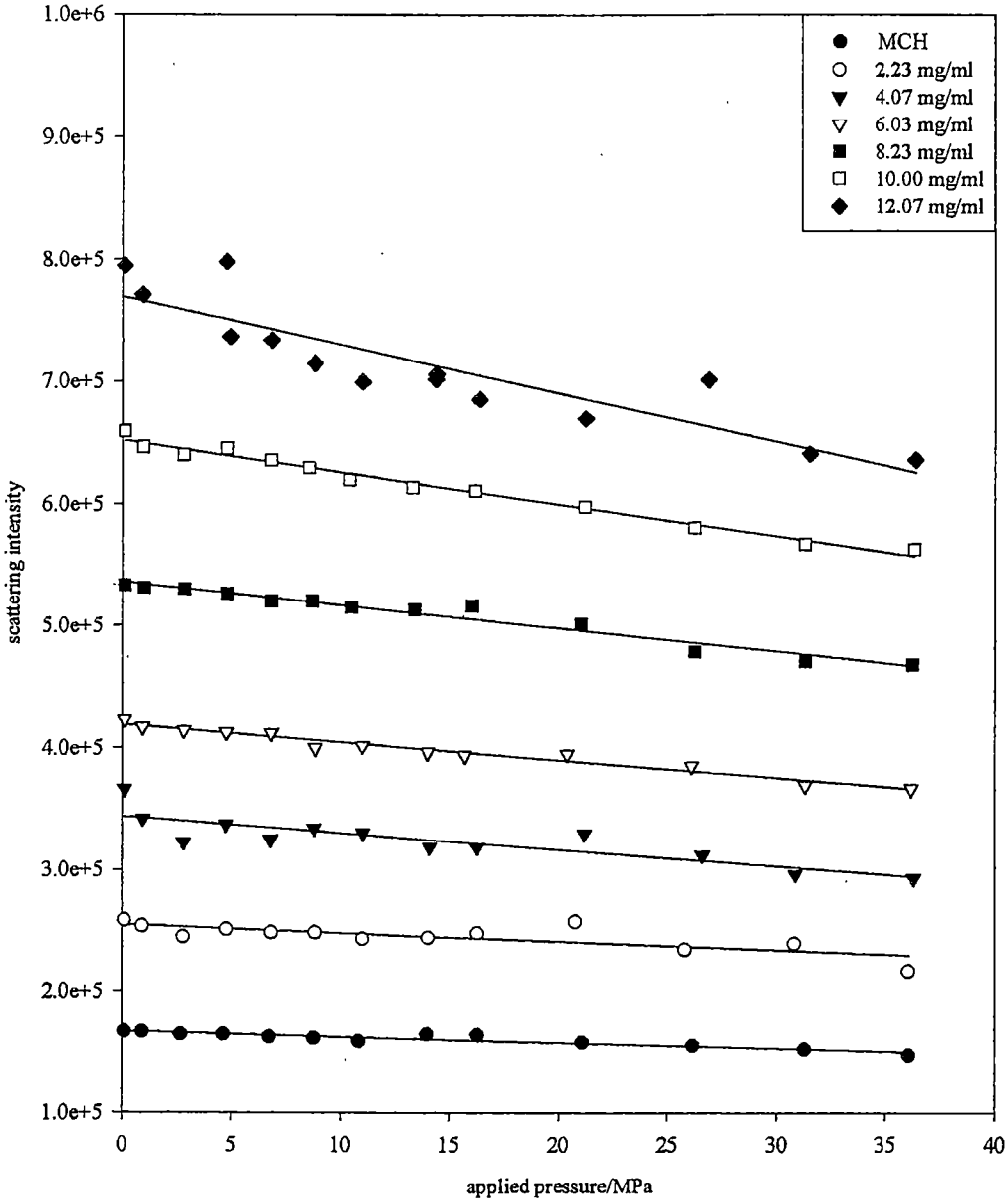

Scattering intensity of PS 25k in MCH at 22 °C as a function of applied pressure

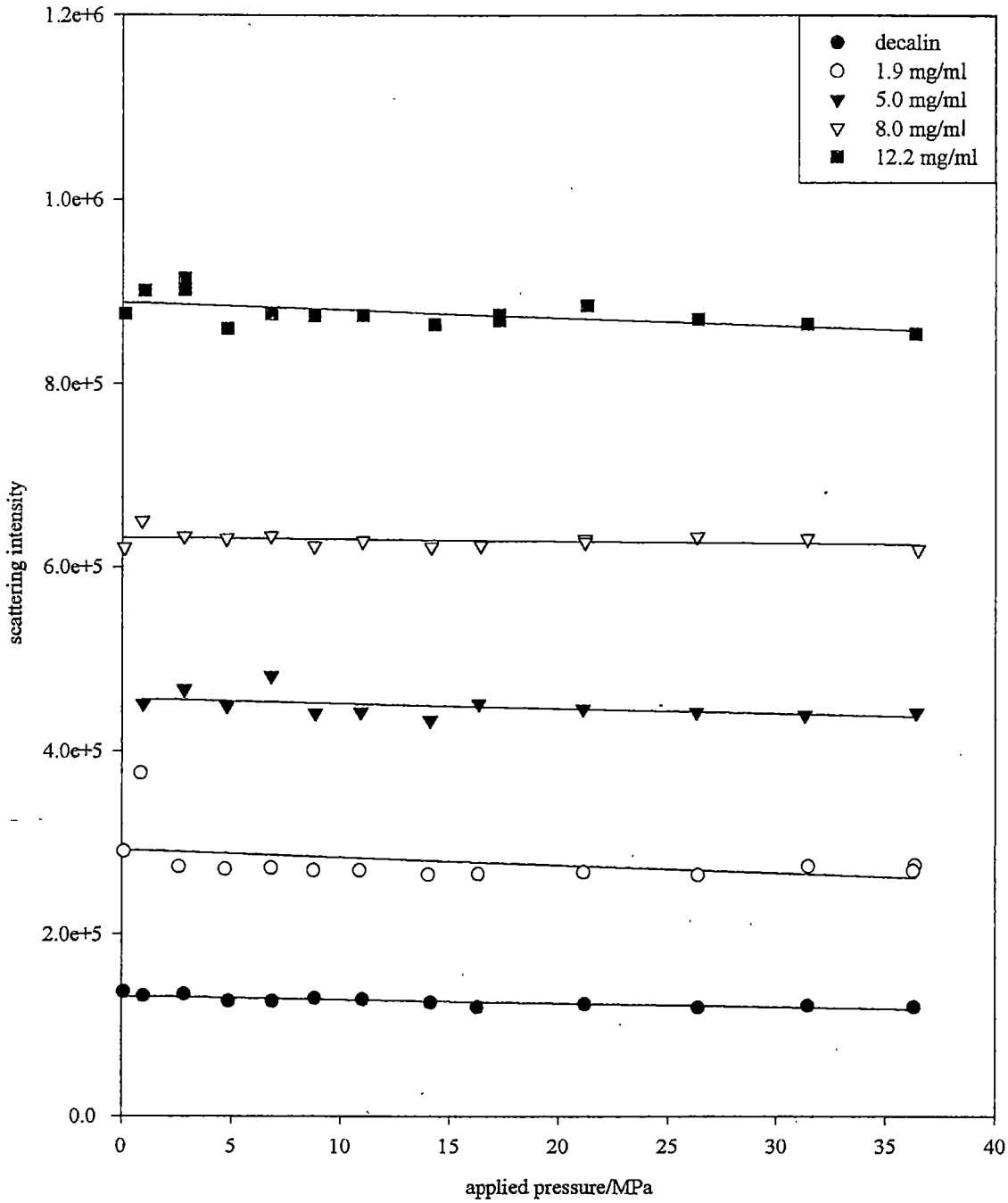

Scattering intensity of PS 90k in decalin at 25 °C as a function of applied pressure

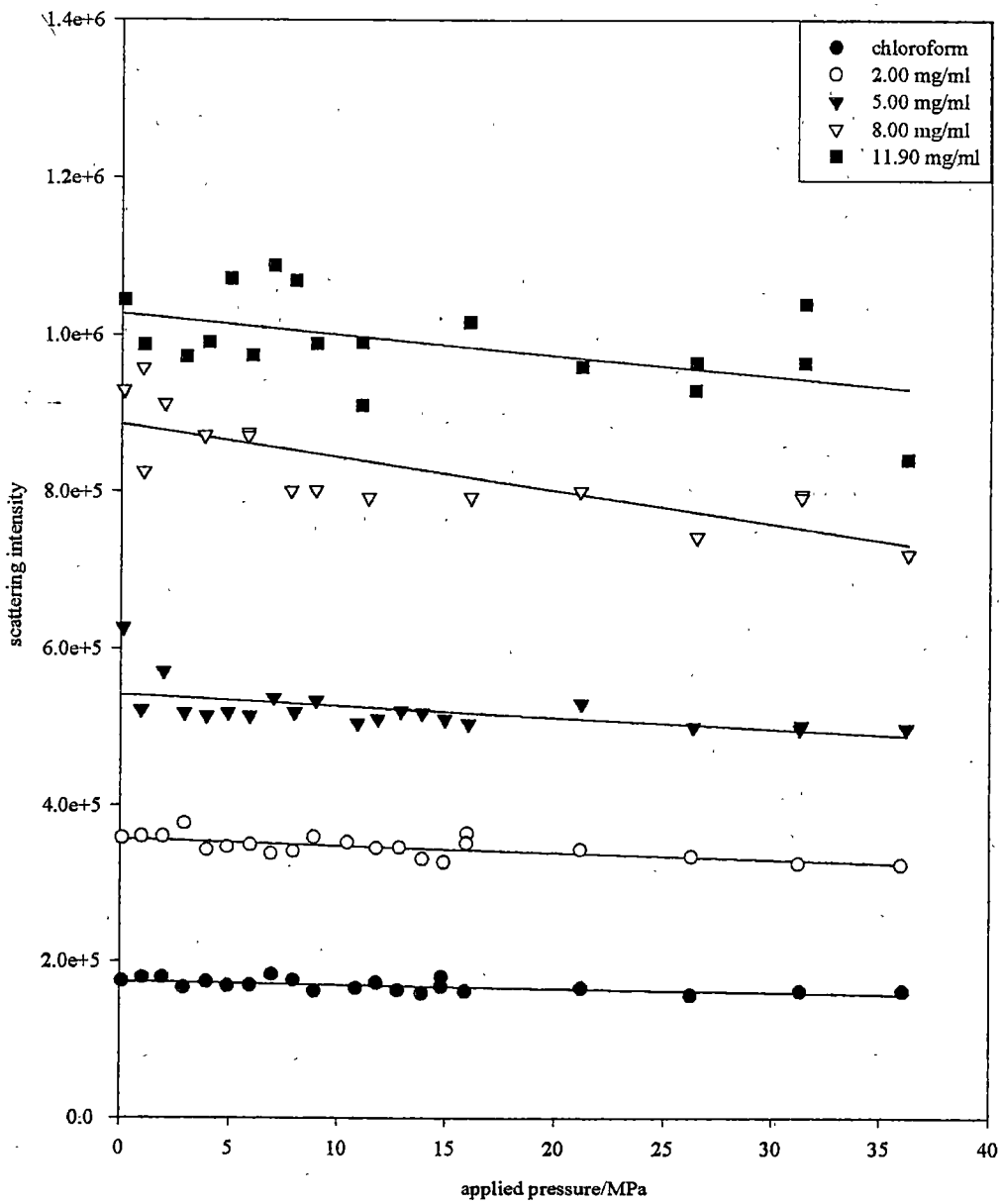

Scattering intensity of PS 90k in chloroform at 25 °C as a function of applied pressure

Vita

Corey Lynn Moses was born to Nelson and Carol Moses in Picayune, Mississippi, on January 19,1969. At age 5, she moved with her family to Pensacola, Florida, where she graduated with honors from Woodham High School in 1987. She graduated *summa cum laude* from Mississippi State University in 1992 with a B.B.A. in marketing and a B.S. in apparel, textiles, and merchandising. Corey then returned to Pensacola to attend the University of West Florida and received a B.S. in chemistry in June 1996. While working toward this degree, she was employed as a cooperative education student at the Joint Oil Analysis Program - Technical Support Center at Naval Air Station, Pensacola, Florida. In August 1996, Corey began graduate studies at the University of Tennessee. She received her Doctor of Philosophy degree in physical chemistry in August 2001 under the direction of Professor Alexander Van Hook. After graduation, Corey accepted a position as an assistant journal editor with the American Chemical Society.